Gondwana Research xxx (2011) xxx–xxx

Contents lists available at ScienceDirect

Gondwana Research

journal homepage: www.elsevier.com/locate/gr

GR focus review

Subduction erosion: Rates, mechanisms, and its role in arc magmatism and the evolution of the continental crust and mantle

Charles R. Stern *

Department of Geological Sciences, University of Colorado, Boulder, CO, 80309-0399, USA

ARTICLE INFO

Article history:
Received 30 November 2010
Received in revised form 23 March 2011
Accepted 27 March 2011
Available online xxxx

Handling Editor: M. Santosh

Keywords:
Subduction erosion
Arc magmatism
Crustal recycling
Mantle evolution
Supercontinent cycle

ABSTRACT

Subduction erosion occurs at all convergent plate boundaries, even if they are also accretionary margins. Frontal subduction erosion results from a combination of erosion and structural collapse of the forearc wedge into the trench, and basal subduction erosion by abrasion and hydrofracturing above the subduction channel. High rates of subduction erosion are associated with relatively high convergence rates (>60 mm/yr) and low rates of sediment supply to the trench (<40 km^2/yr), implying a narrow and topographically rough subduction channel which is neither smoothed out nor lubricated by fine-grained water-rich turbidites such as are transported into the mantle below accreting plate boundaries. Rates of subduction erosion, which range up to >440 km^3/km/my, vary temporally as a function of these same factors, as well as the subduction of buoyant features such as seamount chains, submarine volcanic plateaus, island arcs and oceanic spreading ridge, due to weakening of the forearc wedge. Revised estimates of long-term rates of subduction erosion appropriate for selected margins, including SW Japan (≥30 km^3/km/my since 400 Ma), SW USA (≥30 km^3/km/my since 150 Ma), Peru and northern Chile (50–70 km^3/km/my since >150 Ma), and central (115 km^3/km/my since 30 Ma) and southernmost Chile (30–35 km^3/km/my since 15 Ma), are higher than in previous compilations. Globally, subduction erosion is responsible for >1.7 Armstrong Units (1 AU = 1 km^3/yr) of crustal loss, 33% of the ~5.25 AU of yearly total crustal loss, and more than any one other of sediment subduction (1.65 AU), continental lower crustal delamination (≥1.1 AU), crustal subduction during continental collision (0.4 AU), and/or subduction of rock-weathering generated chemical solute that is dissolved in oceanic crust (0.4 AU). The paucity of pre-Neoproterozoic blueschists suggests that global rates of subduction erosion were probably greater in the remote past, perhaps due to higher plate convergence rates. Subducted sediments and crust removed from the over-riding forearc wedge by subduction erosion may remain in the crust by being underplated below the wedge, or these crustal debris may be carried deeper into the source region of arc magmatism and incorporated into arc magmas by either dehydration of the subducted slab and the transport of their soluble components into the overlying mantle wedge source of arc basalts, and/or bulk melting of the subducted crust to produce adakites. In selected locations such as in Chile, Costa Rica, Japan and SW USA, strong cases can be made for the temporal and spatial correlations of distinctive crustal isotopic characteristics of arc magmas and episodes or areas of enhanced subduction erosion. Nevertheless, overall most subducted crust and sediment, >90% (>3.0 AU), is transported deeper into the mantle and neither underplated below the forearc wedge nor incorporated in arc magmas. The total current rate of return of continental crust into the deeper mantle, the most important process for which is subduction erosion, is equal to or greater than the estimates of the rate at which the crust is being replaced by arc and plume magmatic activity, indicating that currently the continental crust is probably slowly shrinking. However, rates of crustal growth may have been episodically more rapid in the past, most likely at times of supercontinent breakup, and conversely, rates of crustal destruction may have also been higher during times of supercontinent amalgamation. Thus the supercontinent cycle controls the relative rates of growth and/or destruction of the continental crust. Subduction erosion plays an important role in producing and maintaining this cycle by transporting radioactive elements from the crust into the mantle, perhaps as deep as the 670 km upper-to-lower mantle transition, or even deeper down to the core–mantle boundary, where heating of this subducted crustal material initiates plumes and superplumes.

* Tel.: +1 303 492 7170; fax: +1 303 492 2606.
E-mail address: Charles.Stern@colorado.edu.

1342-937X/$ – see front matter
doi:10.1016/j.gr.2011.03.006

Please cite this article as: Stern, C.R., Subduction erosion: Rates, mechanisms, and its role in arc magmatism and the evolution of the continental crust and mantle, Gondwana Res. (2011), doi:10.1016/j.gr.2011.03.006

Contents

1. Introduction

The Earth, as well as being the blue and/or water planet, has also been called the subduction planet. The subduction factory at convergent plate boundaries generates volatile-rich magmas that grow the continental crust, atmosphere and hydrosphere, but subduction also transports components from the atmosphere, hydrosphere and crust back into the mantle, from whence they came (Armstrong, 1981, 1991; Scholl and von Huene, 2007, 2009; Clift et al., 2009a, 2009b; Stern and Scholl, 2010). Subduction erosion, which removes crustal material from the forearc wedge above the lower subducting plate (Fig. 1; von Huene et al., 2004; Clift and Vannucchi, 2004), is the most important process involved in recycling crust back into the mantle associated with the subduction factory, and occurs at all convergent plate boundaries even if they are accretionary margins (Scholl and von Huene, 2007, 2009). Subducted crustal materials may remain in the crust by being underplated below the wedge, or returned to the crust by being incorporated in the source of arc magmas. Alternatively, they may be transported deeper into the mantle, perhaps as deep as the core–mantle boundary, where the D″ layer may be an "anti-crust" derived from former continental and oceanic crust (Komabayashi et al., 2009; Senshu et al., 2009; Yamamoto et al., 2009).

Von Huene and Scholl (1991), in an early review of the process, suggested that subduction erosion, rather than or together with accretion, occurs along 35,300 of the 43,500 km of the total global length of subduction zones along active convergent ocean margins (Fig. 2). They estimated the average rate of subduction erosion to be ~31 km^3/km/my, and the current total world-wide removal rate of upper plate material by subduction erosion as 1.1 Armstrong Units (1 AU = 1 km^3/yr; Kay and Kay, 2008). More recently, Scholl and von Huene (2007, 2009) considered 31,250 km of nonaccreting margins to have an average subduction erosion rate of 42 km^3/km/my, thereby subducting 1.3 AU of crust, and the other 11,000 km of accreting margins to have an average subduction erosion rate of 12 km^3/km/my, thereby subducting 0.1 AU, for a total global rate of 1.4 AU. Clift et al. (2009a, 2009b) independently estimated that globally subduction erosion results in the removal of 1.35 AU of crust. According to their estimates, subduction erosion accounts for ~27% of the total global rate of 4.9 AU of crustal recycling, other processes involved

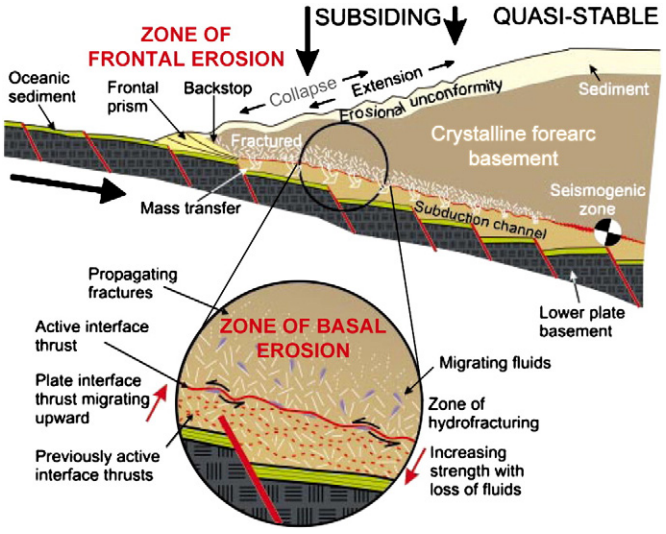

Fig. 1. Cross-section, modified from von Huene et al. (2004), illustrating the components of the forearc wedge and different processes involved in subduction erosion. The subduction channel initially is filled with both oceanic sediment and debris eroded off the forearc wedge surface that accumulates in the frontal prism. Basal erosion results in mass transfer from the bottom of the forearc wedge to the lower plate as dislodged fragments are dragged into the subduction channel. As pore fluid is lost from the sediments in the channel, the strength of coupling between the two plates increases and the seismogenic zone begins.

Please cite this article as: Stern, C.R., Subduction erosion: Rates, mechanisms, and its role in arc magmatism and the evolution of the continental crust and mantle, Gondwana Res. (2011), doi:10.1016/j.gr.2011.03.006

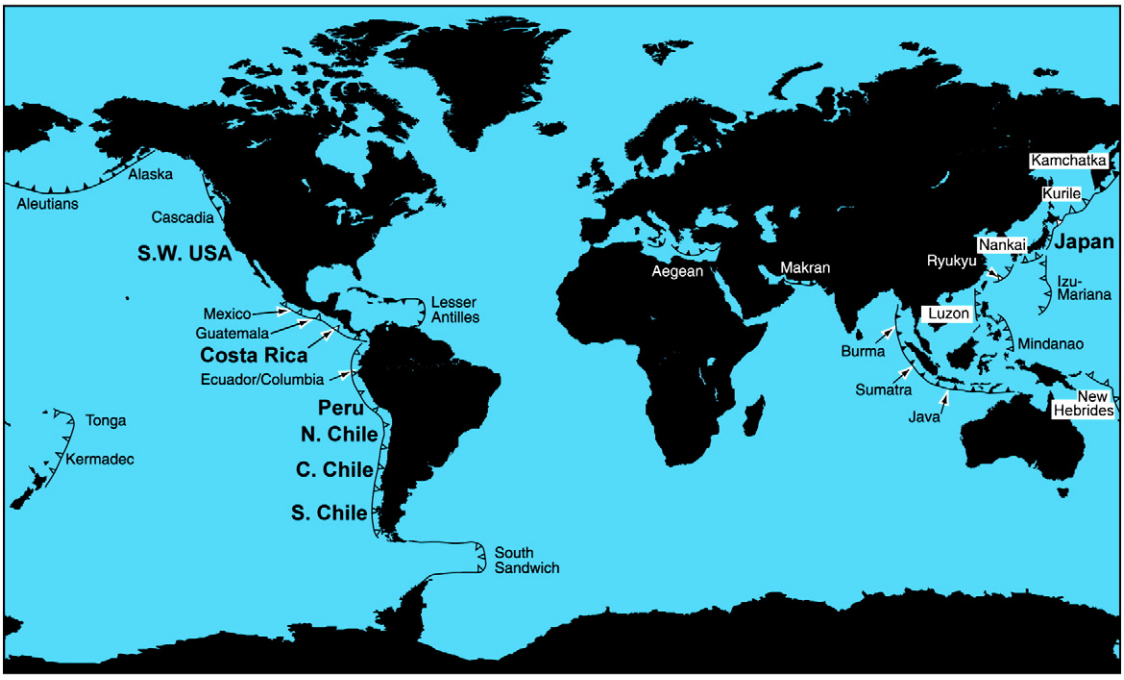

Fig. 2. Global map, modified from Clift and Vannucchi (2004), showing the location of major subduction zones. Subduction erosion occurs at all subduction zones (Scholl and von Huene, 2007, 2009), but those margins where the rates are higher and either no or only a small frontal prisms occur are indicated by open triangles along the trench. These account for 75% of the 42,250 km global length of oceanic trenches. Specific margins addressed in the text are indicated in bold.

being sediment subduction (1.65 AU), continental delamination (1.1 AU), passive margin sediment subduction during continental collision (0.4 AU), and loss of chemical solute (0.4 AU) generated by weathering that is dissolved in subducted oceanic crust. At this rate the entire continental crust could be recycled back into the mantle in ~1.8 Ga (Clift et al., 2009a).

Rates of subduction erosion along different convergent plate boundaries vary significantly (Table 1), up to as high as 440 km^3/km/my (Bourgois et al., 1996), as a function of factors such as convergence rate, sediment supply to the trench, the width of the subduction channel, subduction angle, and the subduction of buoyant features such as spreading ridges, seamounts, juvenile oceanic island arcs, and oceanic fracture zones. Numerous studies have also concluded that subduction erosion is not a steady-state process and that temporal variations in the factors listed above cause short-term variations in the rates of subduction erosion (Bangs and Cande, 1997; Clift et al., 2003; Clift and Hartley, 2007). The rates estimated by von Huene and Scholl (1991), Scholl and von Huene (2007, 2009) and Clift et al. (2009a, 2009b) are therefore only long-term averages for currently active margins, appropriate at most during the last ≤150 Ma. However, the lack of ancient pre-Neoproterozoic blueschists suggests that subduction erosion may have operated at higher global rates in the remote past (Stern, 2005, 2008; Brown, 2008; Condie and Kröner, 2008). Also, Santosh et al. (2009) suggest that during times of continental amalgamation into supercontinents, a combination of subduction erosion and sediment subduction swallows all intervening material "like a black hole" in outer space. Senshu et al. (2009) conclude that the deep subduction in early Earth history, due in part to subduction erosion, of large volumes of continental material rich in K, U, and Th, played a critical role to initiate plumes or superplumes and thus produce and maintain the superplume–supercontinent cycle that more recently in the Earth's history has impacted both mantle dynamics as well as surface processes that result in continental growth, preservation and/or destruction.

This paper reviews geologic evidence for and the estimated rates of subduction erosion, proposed mechanisms for subduction erosion and the factors that affect its rate, and the fate of the eroded material, in particular the extent to which it may be recycled back into the crust through arc magmatism.

Table 1
Revised rates of subduction erosion at selected plate margins.

Arc segment	Length in km	Estimated rates of subduction erosion in km^3/km/my		
		Scholl and von Huene (2007, 2009)	Clift et al. (2009a, 2009b)	This paper
NE Japan	1000	64	120	120
SW Japan	1000	0	0	30
SW USA	600	0	0	30
Peru	2200	70	15	70
Northern Chile (18–33°S)	2200	34	15	50
Central Chile (33–38°S)	500	90	0	115
South-central Chile (38–46°S)	1500	90	0	35
Southernmost Chile (46–54°S)	1000	0	0	30
Total arc length	10,000			
Total eroded per my		427,800	186,000	572,000

2. Geologic evidence for and rates of subduction erosion

2.1. Evidence for subduction erosion

Various lines of geologic and marine geophysical data are interpreted to support subduction erosion. From a geological perspective, subduction erosion has been invoked to explain large amounts of missing continental crust along ocean margins (von Huene and Scholl, 1991) in cases where no evidence exists for regional truncation by strike-slip faulting. Large amounts of continental crust are presumed missing in areas where magmatic arcs have migrated progressively away from the trench axis with time, and where seaward projecting trends in continental basement and/or sedimentary basins are truncated along the coastline. Historically,

Please cite this article as: Stern, C.R., Subduction erosion: Rates, mechanisms, and its role in arc magmatism and the evolution of the continental crust and mantle, Gondwana Res. (2011), doi:10.1016/j.gr.2011.03.006

early suggestions that subduction erosion occurred based on such observations were made along the coast of northern Chile by Rutland (1971) and for northeastern Japan by Murauchi (1971). More recent evidence involves provenance analysis by detrital zircon chronology that documents the partial or complete disappearance of older crustal units as a result of subduction erosion (Grove et al., 2008; Isozaki et al., 2010; Jacobson et al., 2011).

Marine geologic and geophysical evidence for subduction erosion includes the presence in the landward trench wall of crystalline basement rocks which make up the rock framework of the toe of the upper plate wedge, the lack of an older "middle prism" of accreted lower plate sediment (Scholl and von Huene, 2007), and/or only a small (<40 km wide) "frontal prism" of actively deforming sediment in a trench (Fig. 1). Erosive margins have been shown to have bathymetric slopes >3° to as high as 8°, and taper angles >7° to as high as 20°, while accretionary margins generally have bathymetric slopes <3° and taper angles <10° (Clift and Vannucchi, 2004). Also tilted and subsided erosional surfaces, originally formed near sea level and then buried by younger shallow water sediment along an advancing shoreline, as first observed both in the margins of NW Japan and Peru (von Huene and Lallemand, 1990), together are interpreted to indicate forearc subsidence due to subduction erosion.

Rates of subduction erosion have been estimated by 1) determining the amount of loss of fore-arc material, which depends in part on crustal thickness, resulting from the trench retreat rate required to produce migration of the magmatic arc over an extended period of time; 2) accounting for some portion of crustal shortening in balanced cross-sections constructed across deformed arc segments; and 3) by calculating loss of material from the fore-arc wedge based on the amount and timing of subsidence of buried erosional surfaces documented on the landward trench slope by marine geophysical techniques. The latter method, which involves comparing the margins present dimensions with that when subsidence began, is described in some detail by von Huene and Lallemand (1990), von Huene and Scholl (1991), Scholl and von Huene (2007) and Clift et al. (2003).

The combination of the evidence for subduction erosion, and the manner in which this evidence has been used to calculate its rate, can best be evaluated in the context of specific examples of erosive convergent plate margins. This evidence is briefly reviewed below, as a contribution to the estimates of the long-term global rates of subduction erosion (Table 1), for the margins east of Japan and west of the USA, Peru and Chile. Other margins (Fig. 2) have been well documented in the reviews of von Huene and Scholl (1991), Clift and Vannucchi (2004), Scholl and von Huene (2007, 2009) and Clift et al. (2009a, 2009b).

2.2. Japan

von Huene et al. (1982) described a subsided near-shore erosion surface, cut in a late Cretaceous lithified accretionary complex, overlain by late Oligocene conglomerates and sands diagnostic of a near-shore or beach environment, at 2750 m below sea level 90 km landward of the northeastern Japan trench axis. Younger sediment, accumulated in increasingly deeper water, documents the progressive subsidence over 22 my of the erosion surface. Seismic reflection data trace this surface to a depth of >7 km along the lower landward trench slope. Approximately 75 km of landward migration of the trench accompanied this subsidence (von Huene and Lallemand, 1990). The small size of the frontal accretionary prism, only 5% of the volume of pelagic sediment that has entered the trench over the last 65 my, is also evidence of sediment subduction and consistent with the margin being erosive (Scholl and von Huene, 2007).

von Huene and Lallemand (1990) reconstructed the Neogene profile of NE Japan fore-arc wedge, and subtracted the volume of the current wedge, thus calculating that for each km of margin, 1110 km^3 of upper crust had been removed by subduction erosion over the last 22 my. Thus the volume rate of subduction erosion averaged 50 km^3/km/my along 1000 km of the NE Japan margin. Based on this estimate, combined with their estimate of the amount of oceanic sediment being subducted, von Huene and Scholl (1991) suggested that the solid-volume thickness of the subducting material is 1 km, consistent with the ~2 km layer of sediment and debris in the subduction channel seismically imaged beneath the seaward edge of the forearc wedge (von Huene and Cullota, 1989). More recent estimates by Scholl and von Huene (2007, 2009) of 64 km^3/km/my, and by Clift et al. (2009a, 2009b) of 120 km^3/km/my, are both significantly higher than earlier estimates (Table 1).

New geologic interpretations of the formation of Japan imply that subduction erosion has also removed large amounts of continental crust in multiple stages from southwest as well as northeast Japan. Isozaki et al. (2010) suggest that although previously the geotectonic evolution of the Japanese Islands has been explained as a simple one-way process of continental growth toward the Pacific Ocean, based on the zonal arrangement of accretionary belts with oceanward younging polarity, what has been overlooked are some ancient units that existed in the past but are not seen at present (Fig. 3). Their provenance analysis of detrital zircons imaged these "ghost" geologic units and demonstrated that they have already disappeared without evident traces. Specifically, they suggested that early Paleozoic (520–400 Ma) igneous zircon grains in late Paleozoic to Triassic sandstones, and early Mesozoic igneous zircons (290–160 Ma) preserved in late Cretaceous sandstones, were derived from arc plutonic rocks that have been essentially totally removed from the crust of SW Japan. Furthermore, the 100–80 Ma Cretaceous arc, which formed 100–200 km west of the contemporaneous trench, has been tectonically transported eastward and emplaced within 50 km of the accretionary belt formed in this trench, implying ~100 km of shortening in the last <80 my (Fig. 4). This was accomplished by uplift and erosion of the arc above mid-crustal detachments.

Isozaki et al. (2010) conclude that the growth of SW Japan did not proceed uniformly, but was punctuated several times by severe shrinkage due to the subduction of arc crust. They suggest that in order for the older granitic batholiths of Japan to have vanished, there must have been extensive exposure of the batholiths on the surface, followed by rapid erosion, transportation of their detrital grains to the trench and finally subduction into mantle. Even in the case of the widely exposed Cretaceous Ryoke batholith belt in SW Japan, the abundant coeval zircon grains in the Paleogene accretionary belt indicate that a huge portion of the batholith has been eroded (Fig. 4) and presumably in part subducted. Uplift and erosion of this arc, and the previous early Mesozoic and Paleozoic arcs, therefore imply minimum average long-term subduction erosion rates of ≥30 km^3/km/my for 1000 km of trench along SW Japan (Table 1).

2.3. Western USA

Although the current plate boundary between the North American and Pacific plates in the southwestern USA is the San Andreas strike-slip fault, this boundary involved plate convergence and subduction in the Mesozoic and early Cenozoic. The Franciscan subduction complex, Great Valley forearc basin, and Sierra Nevada batholith of central California, located east of the San Andreas fault, are NNW-trending lithotectonic belts interpreted to have been produced during late Mesozoic–early Cenozoic subduction of the oceanic Farallon plate beneath the western edge of North America. In southern California, west of the San Andreas fault, disrupted but similar lithotectonic units include the Pelona–Orocopia–Rand–Catalina schists, fore-arc valley sediments, and volcanic and plutonic rocks of the Peninsula Range batholiths (Fig. 5). Recent $^{40}Ar/^{39}Ar$ thermochronologic analyses and U–Pb dating of detrital zircons of the Pelona–Orocopia–Rand–Catalina schists in southwestern California suggest that the sedimentation and underplating of these subduction complexes occurred from >120 Ma

Please cite this article as: Stern, C.R., Subduction erosion: Rates, mechanisms, and its role in arc magmatism and the evolution of the continental crust and mantle, Gondwana Res. (2011), doi:10.1016/j.gr.2011.03.006

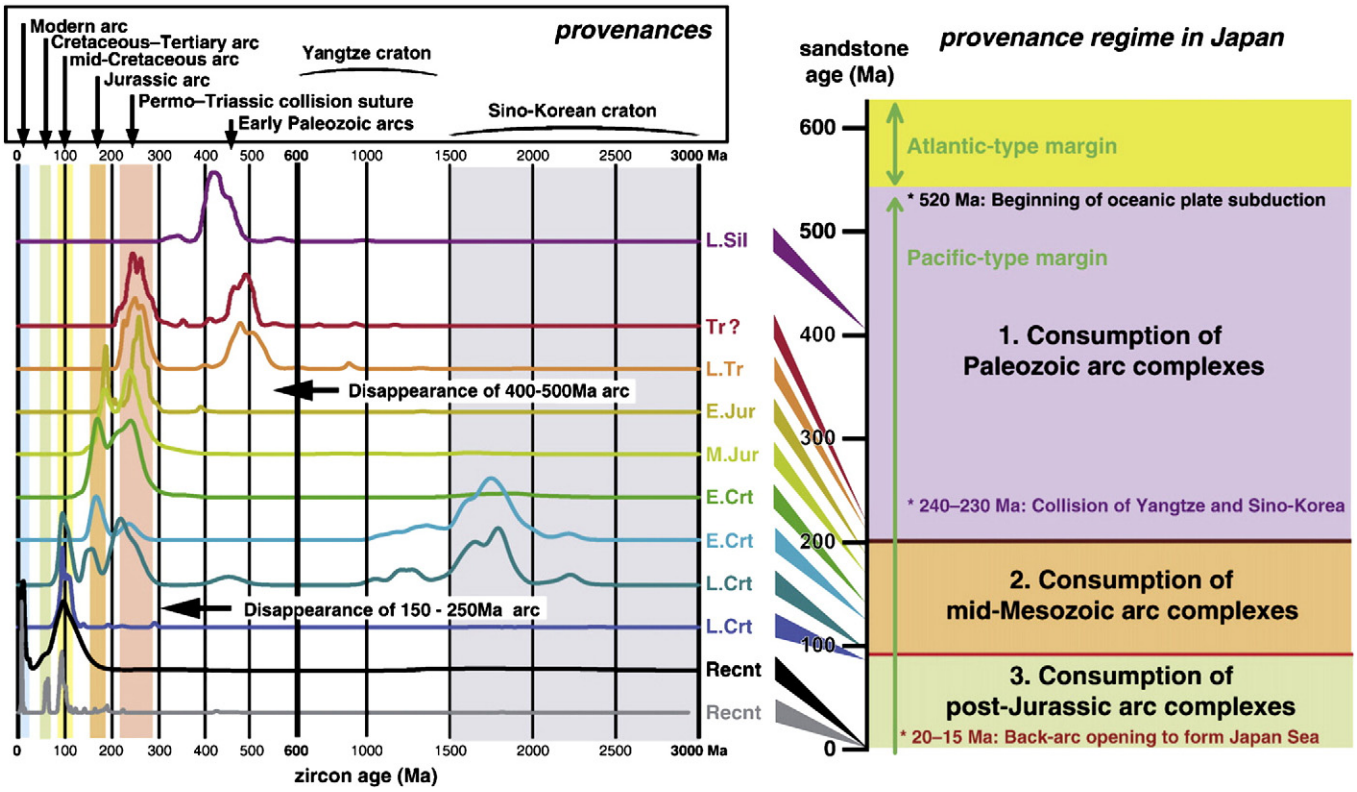

Fig. 3. Plots, from Isozaki et al. (2010), of age spectra of detrital zircon grains from the mid-Paleozoic to Mesozoic sandstones and Recent river sands in Japan, showing secular change in provenances that shed terrigenous clastics to Japan. The figure documents three distinct stages in the over 500 my history of the Japanese Islands in terms of terrigenous clastics from granitic sources, these being before the Late Triassic (ca. 200 Ma), Jurassic to mid-Cretaceous (ca. 200–90 Ma), and after the Late Cretaceous (ca. 90 Ma). During each stage different older sources were consumed by subduction erosion.

to <60 Ma (Jacobson et al., 2000, 2011; Barth et al., 2003; Grove et al., 2003, 2008). The older Catalina schists accreted over a ~20 my period between 122 and 97 Ma (Grove et al., 2003, 2008). The oldest (122–115 Ma) of these metasediments formed from craton-enriched detritus derived largely from pre-Cretaceous wall rock and early Cretaceous volcanic cover of the Peninsula Range batholiths, while the younger units (95–97 Ma) formed from detritus dominated by this batholith's plutonic and volcanic debris generated as it was uplifted and exhumed (Fig. 5). Protolith and emplacement ages for the Pelona–Orocopia–Rand schists, which overlap in age and provenance with the youngest part of the Catalina Schist, decrease from >90 Ma in the northwest to <60 Ma in the southeast. Detrital zircon U–Pb ages imply that metasandstones in the older units of these schists originated primarily from the western belt of the Sierran–Peninsular Ranges arc, while younger units were apparently derived by erosion of progressively more inboard regions, including the southwestern edge of the North American craton.

The Pelona–Orocopia–Rand–Catalina schists are inferred to record an evolution from normal subduction prior to the early late Cretaceous to flat subduction extending into the early Cenozoic (Fig. 5; Grove et al., 2008; Jacobson et al., 2011). The transition from outboard to inboard sediment sources appears to have coincided with removal of arc and forearc terranes. Jacobson et al. (2011) suggest that by 95–90 Ma the Farallon plate had apparently transitioned, at least in southern California, to a more shallow mode of subduction (Fig. 5B), perhaps related to the presence of an aseismic ridge or oceanic plateau (Saleeby, 2003), and that this geometry favored subduction erosion of the overriding North American plate, inboard migration of the axis of arc magmatism, and under-plating of Pelona–Orocopia–Rand–Catalina schists. Over 150 km of fore-arc basin and arc were removed prior to ~60 Ma. Some, but not all of this crustal loss may have been related to strike-slip truncation by the Nacimiento fault, but this fault, which was driven by the subduction of the aseismic ridge, was active only after <75 Ma, so at least modest subduction erosion occurred prior to this time (Jacobson et al., 2011). Early >123 Ma nonaccretionary behavior of the western USA plate boundary has also been documented by Dumitru et al. (2010). Other evidence for subduction erosion along this plate margin prior to 75 Ma includes an average of 2.7 km/my eastward migration of magmatism in the Sierra Nevada batholiths between 120 and 90 Ma (Stern et al., 1981; Chen and Moore, 1982). During the same time period, at ~100 Ma, the magmatic arc that generated the Peninsula Range batholiths shifted abruptly eastward in conjunction with the intrusion of the La Posta tonalite–trondjhemite–granodiorite (TTG) suite (Fig. 5; Grove et al., 2008). The subsequent Maastrichtian to Paleogene regional marine transgression of the Salinian block and adjacent areas may have been related to an isostatic response to removal of material from the North American mantle lithosphere and lowermost crust base by subduction erosion associated with shallow angle Larimide subduction, which may have enhanced existing erosive processes (Grove et al., 2008; Jacobson et al., 2011). Conservatively averaged over the last 150 my, the removal of 150 km of 30 km thick crust implies long-term subduction erosion rates of ~30 km^3/km/my (Table 1) along 600 km of the SW US where convergence is no longer occurring, and much faster rates between 150 and 60 Ma.

2.4. Peru

Seismic reflection data and drill have demonstrated a subsidence history similar to Japan off the west coast of Peru, with an erosion surface, cut in Paleozoic crystalline metamorphic rocks, descending seaward to depths >4 km. The erosion surface is buried below first sandy shallow water deposits of middle Eocene age, and subsequently a Neogene section of middle Miocene and younger sediments accumulated in deeper water. The Neogene sequence has been

Please cite this article as: Stern, C.R., Subduction erosion: Rates, mechanisms, and its role in arc magmatism and the evolution of the continental crust and mantle, Gondwana Res. (2011), doi:10.1016/j.gr.2011.03.006

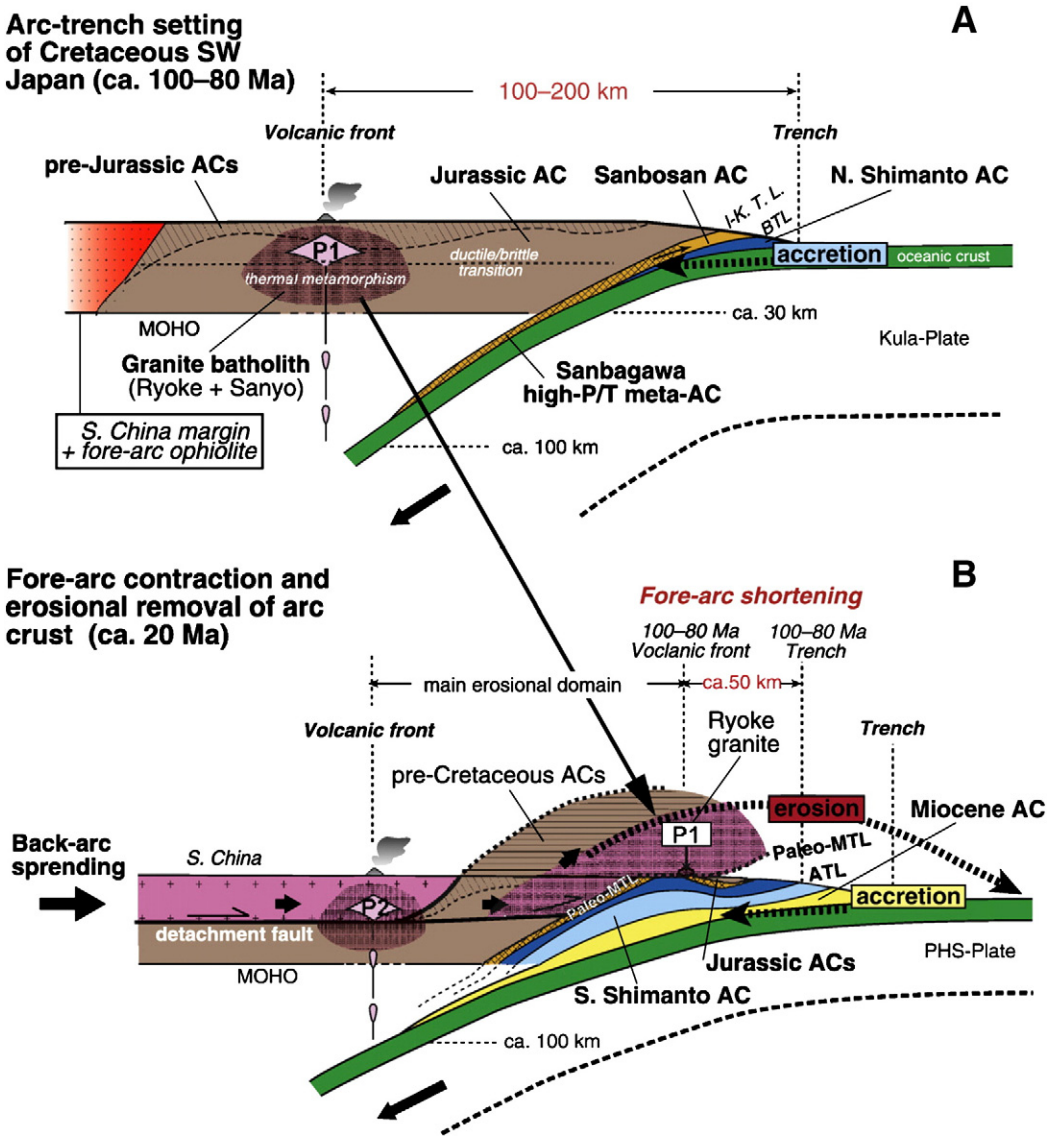

Fig. 4. Simplified model cross-section, from Isozaki et al. (2010), of the Miocene backarc spreading and forearc contraction for juxtaposing the Ryoke granite batholith belt and coeval high-P/T Sanbagawa meta-accretionary complex (AC) in SW Japan. (A) The mid-Cretaceous arc–trench setting of the SW Japan segment in East Asia. Oceanic subduction from the Pacific side produced the Northern Shimanto AC belt next to trench, whereas the Ryoke granite batholith (P1) belt formed beneath the volcanic arc 100–200 km west of the trench. (B) Miocene SW Japan shortened by forearc contraction induced by the opening of the Japan Sea. The upper crust of the arc, including the Cretaceous batholith belt and associated pre-Cretaceous accretionary and meta-accretionary units were horizontally transported oceanward along mid-crustal detachments, resulting in the occurrence of the Ryoke granite batholith unit (P1) over the coeval high-P/T meta-AC belt in western Shikoku. Note that the location of P1 is now only ~50 km from the trench. This forearc shortening was accompanied by severe erosion on the surface to produce a huge amount of terrigenous clastics forming the extensive southern part of the Shimanto AC belt. Also a large amount of clastics was subducted into the deep mantle, and thus the total volume of the Phanerozoic crust of SW Japan decreased by subduction erosion.

affected by an episode of uplift followed by renewed subsidence due to the subduction of the Nazca Ridge below the Peruvian margin (von Huene et al., 1988). Hampel et al. (2004a, 2004b) conclude that the amount of uplift, up to 900 m, is consistent with the high-strength of the Paleozoic crystalline basement that makes up the rock framework of the forearc wedge. The uplift and subsidence related to the subduction of the Nazca ridge have fractured and weakened this rock framework, and Bourgois et al. (1988) interpret seismic reflection data to suggest that the middle continental slope off the coast of Peru is undergoing extension and massive collapse, with the lower slope area consisting in large part of the debris produced by this mass-wasting process.

Rates of tectonic erosion calculated by comparing the volume of the Peru forearc wedge at 20 Ma compared to today indicate removal of 620 km^3/km at a rate of 31 km^3/km/my. However, when calculated over only the last 8 my, which includes the time during which the Nazca Ridge was subducted, the data indicate removal of 370 km^3/km at a rate of 46 km^3/km/my (von Huene et al., 1988; von Huene and Scholl, 1991). This would imply that between 20 and 8 Ma, before the subduction of the Nazca ridge, erosion rates were only 20 km^3/km/my. The increased rate of subduction erosion associated with the subduction of the Nazca ridge has been confirmed by Clift et al. (2003), who estimate that long term subduction erosion caused arc-ward trench retreat of 1.5–3.1 km/my between 47 and 11 Ma, while after 11 Ma trench retreat rates increased to 4.6–9.1 km/my. For 25 km thick crust, this implies a long-term subduction erosion rate of 37–78 km^3/km/my, and short term rates of 115–228 km^3/km/my, both estimates significantly higher those of von Huene et al. (1988). In their more recent review, Scholl and von Huene (2007, 2009) suggest 70 km^3/km/my as the long-term rate over the last 70 my (Table 1), which is consistent with the long-term value based on the extent of the eastward migration of the magmatic arc between the late Cretaceous and the present (Scheuber and Reutter, 1992; Atherton and Petford, 1996). As for Japan, von Huene and Scholl (1991)

Please cite this article as: Stern, C.R., Subduction erosion: Rates, mechanisms, and its role in arc magmatism and the evolution of the continental crust and mantle, Gondwana Res. (2011), doi:10.1016/j.gr.2011.03.006

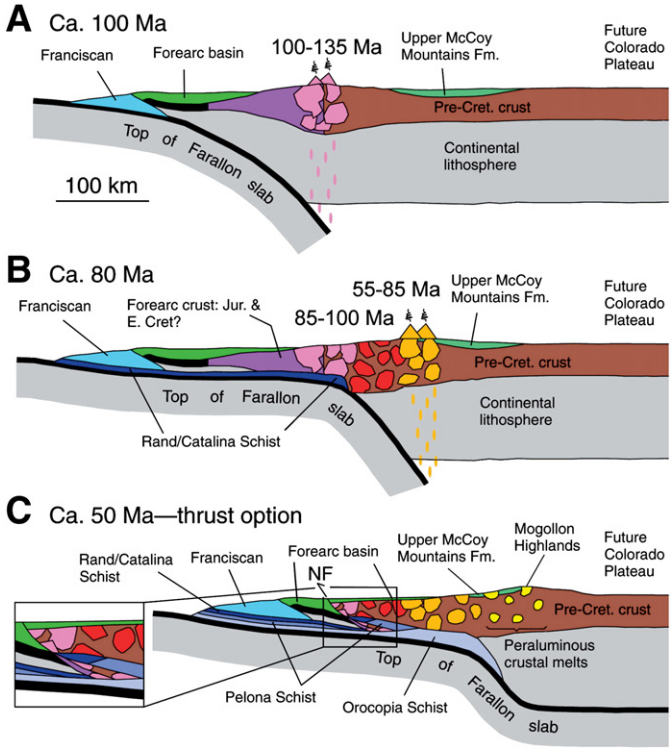

Fig. 5. Tectonic model, from Jacobson et al. (2011), for underplating of the Pelona–Orocopia–Rand–Catalina schists and development of the Nacimiento fault in southwestern USA. (A) Geometry prior to the onset of flat subduction and emplacement of the Pelona–Orocopia–Rand–Catalina schists. (B) Early phase of flat subduction and eastward arc migration preceding initiation of slip on the Nacimiento fault. (C) Relations following cessation of slip along the Nacimiento fault (NF), assuming thrusting. The North American craton is held fixed in all panels. The eastward migration of the trench, the thinning of the forearc crust and the cropping off of the roots of the batholiths as subduction angle decreased all represent different aspects of crustal loss by forearc subduction erosion.

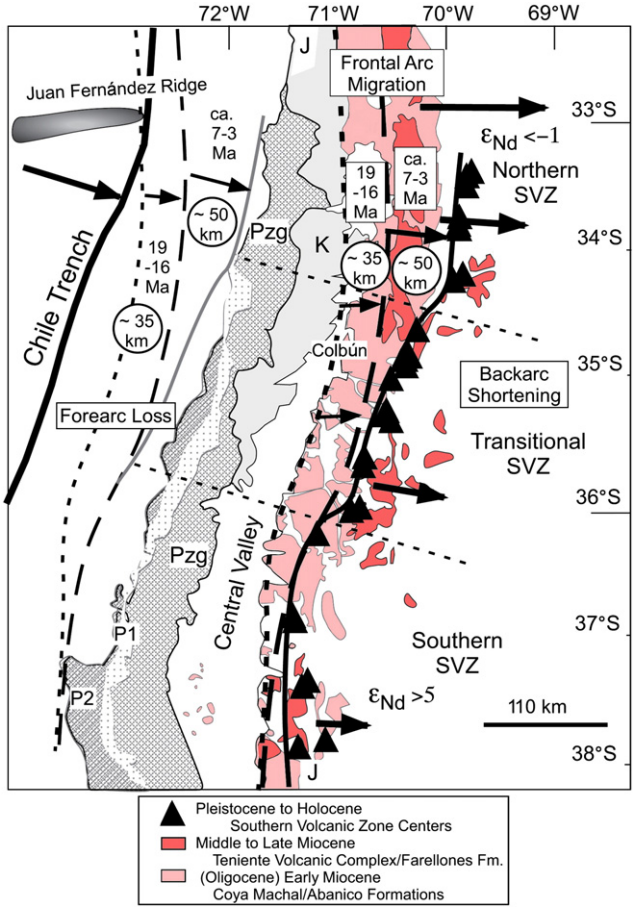

Fig. 6. Regional map, from Kay et al. (2005), of central Chile between ~32°S and 38°S, with lines showing correlations of early Miocene to Holocene arc fronts on land and inferred position of corresponding coastlines offshore. Arrows show relative amounts of frontal-arc migration, forearc loss, and backarc shortening. Northwest–southeast trending dashed lines show offsets in the modern volcanic front that separate the Southern Volcanic Zone (SVZ) into the northern, transitional, and southern segments (Stern et al., 2007). In the active arc region, lines connect outcrop patterns marking early Miocene (pink), middle to late Miocene (red), and SVZ (undashed, connecting Pleistocene to Holocene volcanic centers [triangles]) magmatic fronts. Arrows between the lines indicate inferred distance (given in circles) of frontal-arc migration from 19 to 16 Ma and from 7 to 3 Ma. In the forearc, lines between the trench and the coast show inferred early Miocene (short dashed) and middle to late Miocene (long dashed) coastlines under the assumption that the distance of frontal-arc migration equals the width of missing coast. Arrows between the lines indicate distance (shown in circles) of inferred loss from ca. 19 to 16 Ma. In the backarc, the length and position of arrows show the location and proportional amounts of crustal shortening over the past 20 my inferred from structural profiles. Also shown are other outcrop patterns that have long been used as evidence for forearc subduction erosion along this margin. The first is the northward narrowing and disappearance of the Paleozoic high pressure (P1) and low pressure (P2) paired metamorphic and granitoid (Pzg) belts along the coast (Stern and Mpodozis, 1991). The second is the presence of Jurassic arc rocks (marked by J) along the coast north of 33°S, but inland near the SVZ at ~38°S. K indicates Cretaceous magmatic rocks. ε_{Nd} is >5 for active SVZ volcanoes south of 36°S, and ≤1 for those in the northern SVZ north of 34°S, as a result of increased mantle source region contamination by subducted crust due to the northward increase in the rate of subduction erosion associated with the subduction of the Juan Fernández Ridge at 33°S (Stern, 1991; Stern et al., 2011).

calculate a 1 km subduction channel to accommodate the subducted oceanic sediment and eroded continental debris.

Clift and Hartley (2007) calculated a much slower rate of erosion, of only 15 km^3/km/my during the last 2 Ma, as suggested by a change from long-term subsidence to modest uplift of onshore basins in southern Peru and northern Chile. Clift et al. (2009a, 2009b) use this low rate of subduction erosion for both northern Chile and Peru in their global estimate of the amount of crust currently subducted due to subduction erosion (Table 1), although they conclude that uplift is steepening the landward trench slope and that this style of margin evolution cannot be steady state, and that therefore this rate is actually lower than the average long-term rate.

2.5. Northern Chile (18–33°S)

In northern Chile, Rutland (1971), Kulm et al. (1977) and Schweller and Kulm (1978) suggested subduction erosion to explain the lack of Mesozoic or Cenozoic accretionary complexes and the occurrence of pre-Andean Paleozoic crystalline basement and the Jurassic magmatic arc along the coast. Other geologic evidence for subduction erosion west of northern Chile includes the ~250 km eastward migration of the Andean Jurassic to Cenozoic magmatic belts (Ziegler et al., 1981; Stern, 1991; Peterson, 1999), the northwest strike and almost complete disappearance north of 27°S of the Late Paleozoic Gondwana subduction accretionary complexes that form the Coastal Cordillera in central Chile (Fig. 6; Stern, 1991; Stern and Mpodozis, 1991), and shortages in the amount of crustal shortening that can be accounted for by crustal area balance calculations (Stern, 1991; Schmitz, 1994; Allmendinger et al., 1997). Also, the Upper Triassic Cifuncho Formation, which occurs along the coast of northern Chile at 25.5°S, consists of terrigenous conglomerates and sandstones derived from a Paleozoic source once located to the west off the current coast, but which is now nowhere to be found (Suárez and Bell, 1994).

Marine geologic and geophysical data that imply subduction erosion along the trench axis west of northern Chile include the observation of the almost complete lack of a prism of deformed sediment in the trench (Kulm et al., 1977), and the interpretation that

Please cite this article as: Stern, C.R., Subduction erosion: Rates, mechanisms, and its role in arc magmatism and the evolution of the continental crust and mantle, Gondwana Res. (2011), doi:10.1016/j.gr.2011.03.006

the small (15–20 km wide) frontal prism in the trench consists dominantly of debris from the gravitational failure of the forearc lower slope (von Huene and Ranero, 2003; Sallarés and Ranero, 2005), which dips at 9° into the trench and is undergoing extension (Hartley et al., 2000). von Huene and Ranero (2003) and Sallarés and Ranero (2005) document a 1.5 km wide subduction channel. Sallarés and Ranero (2005) suggest that grabens in the down-bending oceanic crust actually deepen in relief under the forearc, collecting material eroded from the base of the wedge by hydrofracturing, but that by 25 km depth the subduction channel has largely lost its fluids and the subducting plate becomes more strongly mechanically coupled to the overlying plate.

Based on the observed ~250 km eastward migration of the volcanic arc over the last ~200 my between 20 and 26°S, and a crustal thickness along the coast of ~40 km, Stern (1991) calculated subduction erosion rates of 50 km^3/km/my (Table 1). von Huene et al. (1999) and von Huene and Ranero (2003) calculated rates of 56 and 45–50 km^3/km/my, respectively, based on an estimation of the void volume of the horsts in the down-going slab. Kukowski and Oncken (2006) calculated lower rates of 40–45 km^3/km/my. Scholl and von Huene (2007, 2009) use similar values of 28–40 km^3/km/my for northern Chile in their global estimates of subduction erosion rates (Table 1).

Further to the south, at 30°S, Allmendinger et al. (1997) estimate 165 km of E–W shortening in the past 15 my, and suggest that only 80% of this can be accounted for by sectional balancing. This implies 33 km of unaccounted crust that may have been lost due to subduction erosion. Based on a crustal thickness of 38 km, Stern (1991) calculated a subduction erosion rate of 84 km^3/km/my, and attributed this enhanced rate to both subduction of the Juan Fernández Ridge below this region combined with decreasing subduction angle associated with subduction of this ridge beginning in the middle Miocene. Kay and Coira (2009) also conclude that subduction of the Juan Fernández ridge was a dominant factor in controlling decreasing slab dip below northern Chile during the Miocene, the lowering of which may increase rates of subduction erosion. Since the locus of subduction of this ridge migrated from north-to-south below northern Chile beginning at ~23 Ma (Yáñez et al., 2001, 2002), enhanced short term rates of subduction erosion probably occurred along the coast of northern Chile, just as slower rates of erosion have occurred in the last 2 Ma (Clift and Hartley, 2007), and neither the short- nor the long-term rates reflect steady-state processes.

2.6. Central Chile (33–46°S)

Clift et al. (2009a, 2009b) consider the margin of central and southern Chile to be accreting. However, this only reflects the recent increased sediment flux into the trench due to continental glaciations beginning in the Pliocene (Bangs and Cande, 1997; Kukowski and Oncken, 2006). The central Chile margin actually experienced subduction erosion since at least the late Oligocene (Stern, 1989; Kay et al., 2005). Scholl and von Huene (2007, 2009) suggest an average rate of tectonic erosion of 90 km^3/km/my for the margin of central Chile over the last 20 my (Table 1).

The available information actually suggests along-strike changes in subduction erosion rates towards the south away from the locus of subduction of the Juan Fernández ridge (Fig. 6; Stern, 1989, 1991; Kay et al., 2005; Kukowski and Oncken, 2006). The Juan Fernández Ridge, a ~900 km long chain of seamounts with a mean crustal thickness ≥25 km and a width of ~100 km (von Huene et al., 1997; Yáñez et al., 2001, 2002; Laursen et al., 2002) is currently being subducted below central Chile at 33°S. Because of the geometry of this seamount chain, its locus of subduction has migrated southward along the coast of northern Chile, beginning at ~23 Ma, and reaching its current position at ~10 Ma (Yáñez et al., 2001, 2002). This produced the area of low angle subduction between 27 and 33°S, resulting in migration far to the east of the zone of contractional deformation (Jordan et al., 1983) and the location of the magmatic arc (Kay and Mpodozis, 2002).

Where the ridge disappears below the continental crust of the landward wall of the trench, the forearc is uplifted along the Punta Salinas Ridge. The subducted eastward extension of the ridge coincides with a line of increased earthquake activity which extends down the subduction zone for >400 km. North of the ridge, where the trench takes a landward step (Laursen et al., 2002), the trench is free of sediment, while to the south in contains 2.5 km of continental turbidites transported northward from further to the south. Subsidence has occurred in the Valparaiso basin south of where the ridge enters the trench, suggesting a rate of subduction erosion of 96–128 km^3/km/my for the last 10 Ma (Laursen et al., 2002; Kukowski and Oncken, 2006). Kukowski and Oncken (2006) attribute this to widening of the subduction channel and weakening of the rock framework of the forearc wedge due to the subduction of the ridge.

Beginning at about 10 Ma, compression and uplift due to ridge subduction affected the region south east of 33°S (Skewes and Holmgren, 1993; Kurtz et al., 1997), and a combination of decreasing subdcution angle and subduction erosion has resulted in an ~50 km eastward migration of the magmatic arc since the Pliocene at 33°S (Fig. 6; Stern, 1989; Kay et al., 2005). This corresponds to a maximum subduction erosion rate of 230 km^3/km/my. However, arc migration is less significant further south, and none occurs south of 38°S (Fig. 6; Stern, 1989), suggesting that this is the southern limit of forearc loss related to the subduction of the Juan Fernández ridge at 33°S. Therefore the average subduction erosion rate for the region between 33 and 38°S is ~115 km^3/km/my (Table 1).

According to Kay et al. (2005), an earlier episode of eastward arc migration caused by subduction erosion had occurred between 16 and 19 Ma (Fig. 6) over a larger north-to-south region. These events together have caused the narrowing, north of 38°S, and disappearance north of 33°S, of the Paleozoic lower pressure (P1) and high pressure (P2) paired metamorphic belts and granitoids (Pzg) that accreted along the west coast of Gondwana (Stern and Mpodozis, 1991). Subduction erosion may have also operated south of 38°S prior to the Pliocene as indicated by extension and subsidence of fore-arc basins beginning in the early Miocene (Melnick and Echtler, 2006), although, glacial sediments have filled the trench south of 38°S with sediment in the last 5 Ma (Bangs and Cande, 1997). Kukowski and Oncken (2006) calculate a rate of subduction erosion of 25–35 km^3/km/my from 33 to 46°S between 11 and 3 Ma, slower than that further to north, but still significant. Although the current volcanic arc in central–south Chile occurs over Cretaceous age plutons, the truncation of the forearc wedge by subduction erosion is consistent with the fact that considerable forearc extension, during the event that formed the Chilean Central Valley between 33 and 46°S, took place in the wedge during the late Oligocene to early Miocene (19–29 Ma; Muñoz et al., 2000). Therefore a subduction erosion rate of 35 km^3/km/my between 38 and 46°S is considered appropriate (Table 1).

2.7. Southernmost Chile (46–52°S)

Both Clift et al. (2009a, 2009b) and Scholl and von Huene (2007, 2009) consider the >1000 km margin of southernmost Chile to be accreting, but on the average, over the last 14 my, subduction erosion has occurred as the locus of subduction of the Chile Rise, the subduction of which produces very high erosion rates, has migrated from south-to-north. In southern Chile the Chile Rise, an active spreading ridge segmented by numerous fracture zones, is currently being subducted below the continental margin at 46°S (Fig. 7A; Cande and Leslie, 1986). Bourgois et al. (1996, 2000) describe the geologic events associated with the subduction, below the uplifted Taitao Peninsula, of ridge segments to the south and north of the Tres Montes FZ (TMFZ). Between 5 and 4 Ma the ridge segment south of the TMFZ

Please cite this article as: Stern, C.R., Subduction erosion: Rates, mechanisms, and its role in arc magmatism and the evolution of the continental crust and mantle, Gondwana Res. (2011), doi:10.1016/j.gr.2011.03.006

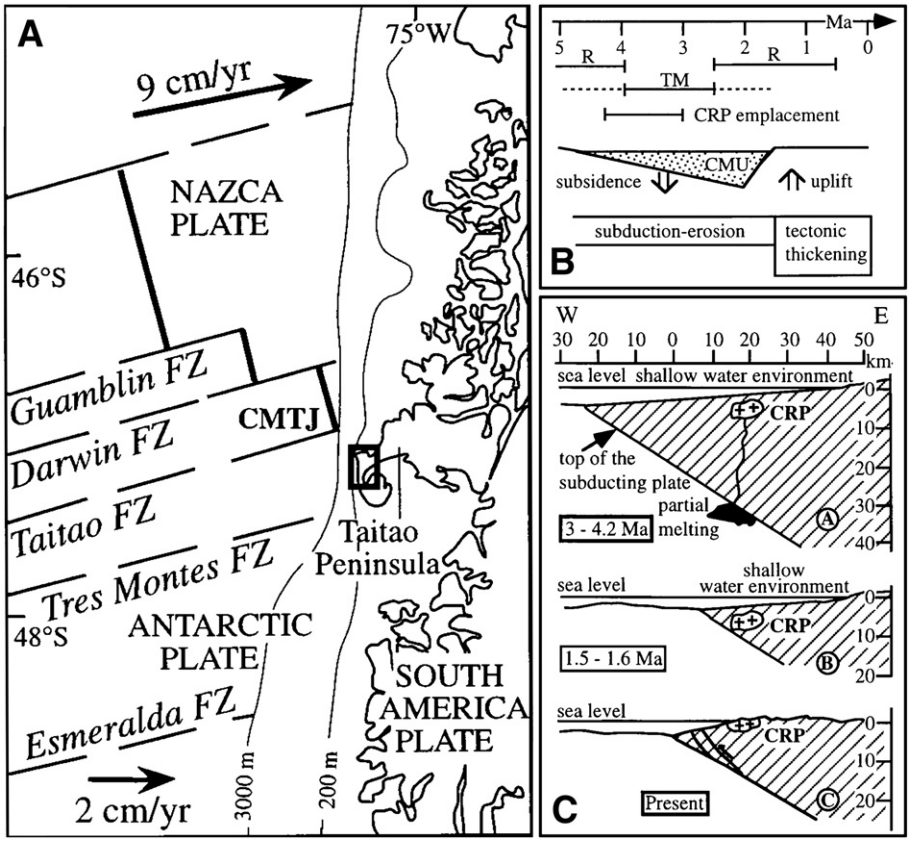

Fig. 7. (A) Location map of Taitao peninsula in southern Chile. FZ = fracture zones; heavy line is the axis of Chile spreading ridge; CMTJ = Chile margin triple junction. (B) Migration of Chile ridge and fracture zones beneath the Taitao peninsula correlates with Cabo Raper pluton (CRP) emplacement, subsidence, and subduction–erosion at depth. CMU = Chile margin sedimentary unit; R = Chile ridge; TM = Tres Montes FZ. (C) Tectonic evolution of Chile margin along Taitao peninsula transect during past 3–4.2 my, modified from Bourgois et al. (1996, 2000), illustrating eastward migration of the trench axis due to rapid subduction erosion, and uplift and exposure of the CRP and CMU.

migrated eastward under the peninsula, followed from 4 to 2.5 Ma by the subduction of the TMFZ itself, and subsequently from 2.5 to 1.5 Ma the subduction of another short ridge segment north of the TMFZ (Fig. 7B). During this time period, subsidence due to subduction erosion lead to the development of 4–6 km of shallow water sediment, which forms the now uplifted and exposed Chile Margin Sedimentary Unit (CMSU; Fig. 7B).

Between 4.2 and 3.0 Ma, the trondhjemitic Cabo Raper pluton (CRP) formed (Fig. 7B). This pluton has chemistry consistent with melting of subducted oceanic crust and sediment metamorphosed to garnet–amphibolite facies at a depth of >30 km. It currently occurs along the coast, only 14 km above the subducted slab (Fig. 7C). To account for the change in depth to the top of the slab, Bourgois et al. (1996) propose 23 km of trench retreat, removing 625 km^3 of rock in the 1.5 to 2.7 million year period between the formation of the pluton and the final subduction of the ridge segment north of the TMFZ, which terminated at 1.5 Ma. After this time, subduction erosion ceased and the plate margin was uplifted, exposing both the CMSU and the CRP. This implies a rate of subduction erosion between 231 and 416 km^3/km/my.

Similar processes have taken place even more recently where the current triple junction occurs northwest of the Taitao Peninsula. Low silica dacites, with ages <2.2 Ma to as young as 70 ka, have been dredged from the Chile trench wall and Taitao ridge just south of the current triple junction (Fig. 8A). These have chemical features similar to the trondhjemitic Cabo Raper pluton, suggesting generation by melting of subducted oceanic crust and sediment at depths between 25 and 45 km (Guivel et al., 1999, 2003). Currently these rocks occur 8 km landward of the trench and only a few kilometers above the down-going slab. Guivel et al. (2003) estimate that this is the result of 44 km of trench retreat in the last 1 million years (Fig. 8B), greater than the higher estimate of Bourgois et al. (1996).

These high rates of subduction erosion may in part reflect the fact that the Chile ridge and the fracture zones that segment it are being subducted at an angle to the trench, so that the triple junction actually moved back (south) and forth (north) as a first fracture zone and then a ridge segment were subducted. Lagabrielle et al. (2000, 2004) suggest that this creates a 'blowtorch' effect (DeLong et al., 1979), heating the subducted slab to the high temperatures (>650 °C) required for melting at relatively shallow depths. It also acts to cyclically uplift and down-drop the overriding forearc wedge, resulting in its fracturing, and thereby enhancing the rates of both frontal and basal subduction erosion.

The rates of subduction erosion calculated for the area close to the Chile ridge-trench triple junction only affect approximately 70 km of the landward trench wall at any one time since the ridge segments being subducted are short and at an angle to the trench, and this affect only lasts 1–3 my because the segments are not separated by great distances. Due to the angle at which the Chile ridge impinges on the trench, the locus of its subduction has migrated ~1000 km from south-to-north between 54 and 46°S over the last ~15 Ma, or 67 km/my. This rate of migration is consistent with the high rates of subduction erosion observed in the vicinity of the current triple junction having sequentially affected 70 km segments of the landward trench wall for a ~1 my period over the last 15 Ma. Therefore the average long-term rate of subduction erosion along the entire 1000 km section of the southernmost Chile trench can be calculated as 30 km^3/km/my (Table 1) using the value 450 km^3/km/my determined by Guivel et al. (2003) for the 60 km of trench close to the present triple junction over the last 1 Ma. Cande and Leslie (1986) note that the western margin of the Mesozoic and Cenozoic Patagonian batholith is significantly closer to the trench south of compared to north of the ridge-trench triple junction, an effect they

Please cite this article as: Stern, C.R., Subduction erosion: Rates, mechanisms, and its role in arc magmatism and the evolution of the continental crust and mantle, Gondwana Res. (2011), doi:10.1016/j.gr.2011.03.006

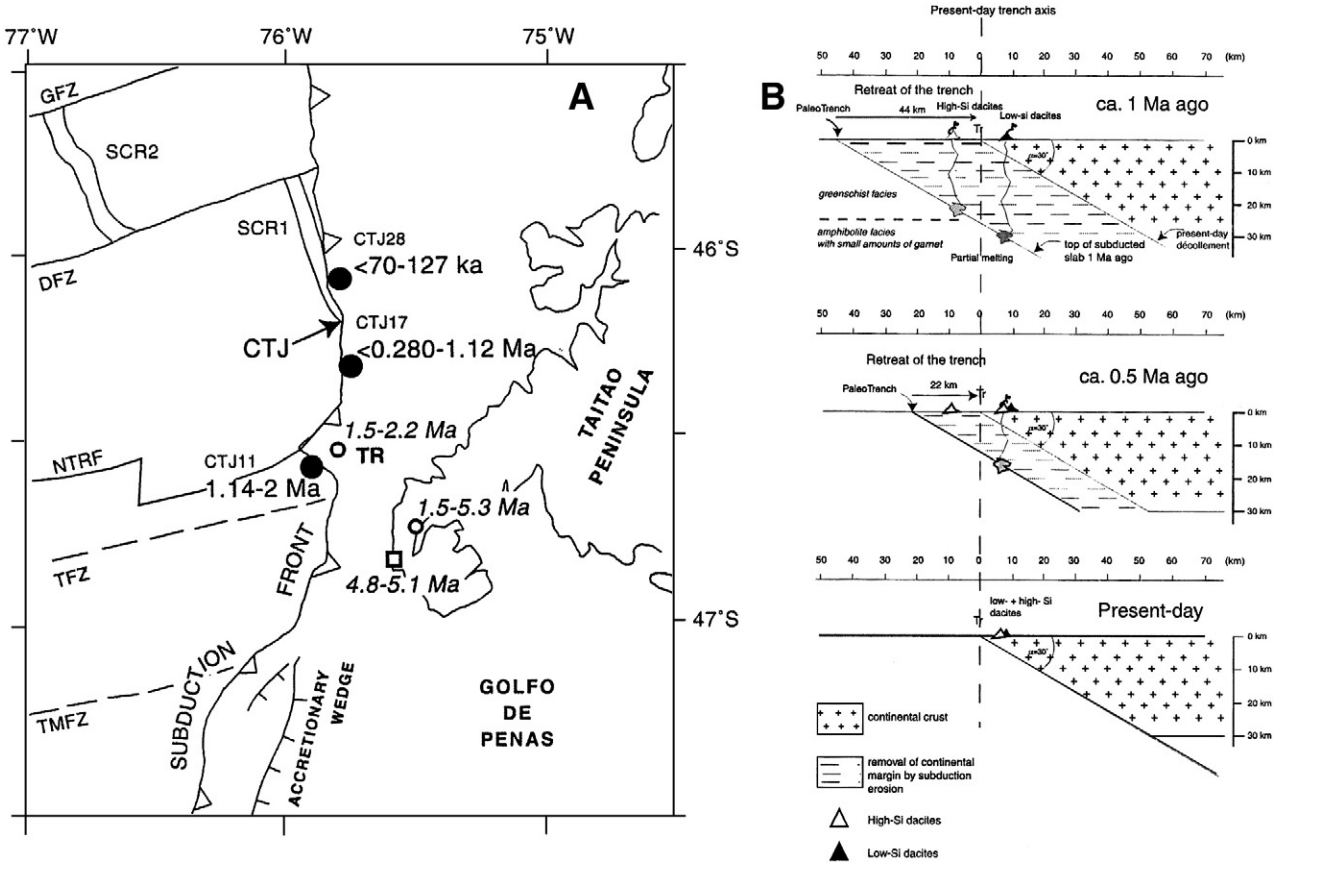

Fig. 8. (A) Map, from Guivel et al. (2003), of the location and age of Pliocene and Quaternary calc-alkaline magmatic rocks in the vicinity of the Chile Triple junction (CTJ). SCR1 and SCR2 are segments of the Chile Ridge offset by various fracture zones. TR is the Taitao fore-arc ridge. (B) Cross-sections illustrating the conditions of shallow slab melting to produce low- and high-silica dacites found in the off-shore area near the Chile Triple Junction, and a geodynamic model involving high rates of subduction erosion (44 km in 1 my) to bring these igneous rocks to their current near-trench axis position on the Taitao ridge.

attribute to subduction erosion related to ridge subduction as the triple junction migrated progressively to the north.

2.8. Summary

Previous reviews have generally been conservative and have underestimated average long-term (20–150 my) rates of subduction erosion at some specific plate boundaries (Table 1), and therefore also underestimated long-term global rates of subduction erosion. Combining the higher rates estimated in this review with the rates Clift et al. (2009a, 2009b) determined at other plate boundaries not addressed here adds a total of 386,000 km^3/my to their calculation of total sediment recycled by subduction erosion per year (Table 1), increasing the global annual estimate to >1.7 AU. This higher revised value makes subduction erosion the single most important factor in their calculations of the rates of global recycling of continental crust into the mantle.

3. Mechanism and factors affecting the rates of subduction erosion

3.1. Frontal and basalt subduction erosion

Subduction erosion occurs by both frontal erosion along the top of the forearc wedge, and by subcrustal basal erosion along the underside of the wedge (Fig. 1; von Huene and Scholl, 1991). Together these processes thin and reduce the volume of the wedge above the subducting plate. A number of mechanisms have been proposed for producing subduction erosion and more than one mechanism may be involved. An early proposal by Hilde (1983) was that roughness in the subducting plate, generated by the formation of horst and graben structures resulting from the down-bending into the trench of the subducting oceanic plate, rasped material by high-stress abrasion from the overlying wedge. However, seismic images indicate that the roughness related to down-bending of the slab may be smoothed due to the infill of these structures by sediment, and the thrust boundary between the subducting slab and overlying wedge generally occurs 1–2 km above the top of the oceanic plate, the two plates being separated by a subduction channel.

Nevertheless, the subduction of horsts and grabens alternatively raises and lowers the base of the fore-arc wedge, fracturing and weakening the rock and sediment that form the wedge, and thus enhancing subduction erosion along the toe of the forearc wedge by causing break-up of the lower trench slope and debris slumping into the trench axis (Fig. 1). Also, at sediment starved trenches, the subduction of unfilled grabens below the toe of the wedge is thought to promote collapse of the lower landward trench slope. Basal erosion proceeds by a combination of these processes as well as hydrofracturing due to fluid overpressure in and above the subduction channel. Ranero and von Huene (2000) have imaged detachment of large lens-shaped masses below the Costa Rican forearc. Wells et al. (2003) suggest that great subduction zone earthquakes affect significant amounts of basal subduction erosion.

3.2. Subduction of buoyant features

Subduction of buoyant features such as ridges, seamounts and oceanic island arcs may result in direct contact, without any sedimentary interface, between the crust of the wedge and the subducting oceanic plate. Furthermore, subduction of buoyant features act to first uplift and subsequently down-drop the overlying

Please cite this article as: Stern, C.R., Subduction erosion: Rates, mechanisms, and its role in arc magmatism and the evolution of the continental crust and mantle, Gondwana Res. (2011), doi:10.1016/j.gr.2011.03.006

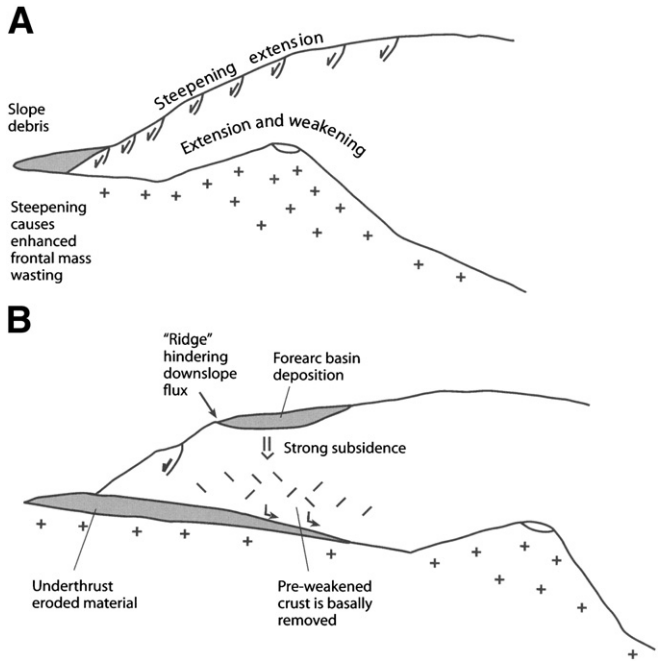

Fig. 9. Sketch, modified from Kukowski and Oncken (2006), illustrating how subduction erosion is enhanced (A) during, and (B) after seamount subduction.

wedge much more significantly than the subduction of the horsts and grabens formed by down-bending of the oceanic plate (Fig. 9). This causes fracturing of the rock framework of the fore-arc wedge, enhancing the possibility for hydrofracturing due to fluid overpressure in the subduction channel, and also results in a reduction of strength contrast between the wedge and the subduction channel, which has been identified in experiments as a factor facilitating basal subduction erosion (Kukowski and Oncken, 2006). As buoyant features are subducted, tectonically eroded sediments are also subducted, which enhances fault-zone fluid content (Bangs et al., 2006), and thus basal erosion by hydrofracturing. Finally, subduction of these features may widen the subduction channel, thereby allowing more rapid transport of sediment and debris in the trench. Where buoyant features have been subducted, reentrant scars and cusps in the regional trend of the trench axis are evidences of enhanced subduction erosion rates (Cande and Leslie, 1986; Laursen et al., 2002; von Huene et al., 2004).

3.3. Factors affecting rates of subduction erosion

Rates of subduction erosion depend fundamentally on the rates of plate subduction, the width of the subduction channel, the supply of sediment to the trench, subduction angle, and the impact of subduction of buoyant features which may widen the subduction channel and weaken the fore-arc wedge. When orthogonal plate convergent rates are relatively high (>60 mm/yr) more sediment can be transported down the subduction channel, and Clift and Vannucchi (2004) suggest that accretion only occurs at margins with relatively slow orthogonal convergence rates (<76 mm/yr). If sediment supply to the trench is high, the channel becomes clogged with sediment, so that trenches with high rates of incoming sediment (>40 km^2/yr) result in accreting margins, while trenches with low rates of sediment delivery (<40 km^2/yr) are erosive. The thickness of sediment in a trench is a function of both the rate of delivery of sediment to the trench and the rate of orthogonal convergence, so that trenches with thin sediment thickness <1 km, which are in all cases erosive (Fig. 10A), have both higher convergence rates and lower sediment supply to the trench, while trenches with thicker sediment layers >1 km, which are generally accretionary, occur at margins with both

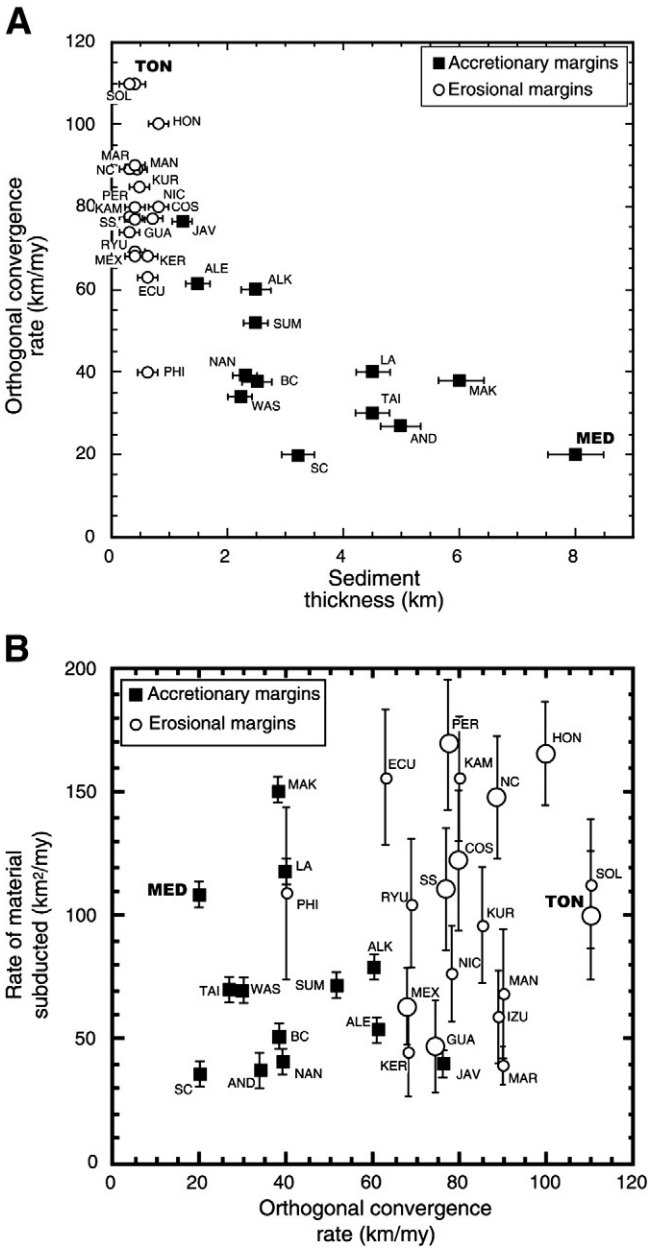

Fig. 10. Plots, from Clift and Vannucchi (2004), of (A) sediment thickness at the trench related to the velocity of the plate convergence, and (B) the relationship between the rate of material subducted below the forearc in both accretionary and erosive plate margins versus the convergence rate. Large circles show erosive plate margins for which a trench retreat is well defined, compared to the small circles representing margins for which tectonic erosion rates are inferred. Note that the same amount of sediment (~100 km^2/yr) is being subducted below the Mediterranean Sea margin (MED; Kopf, 1999; Kopf et al., 2003), at a rate of orthogonal convergence of 20 mm/yr, as is being subducted below Tonga (TON; Clift et al., 1998), at a rate of orthogonal convergence of 110 mm/yr, which can only be accomplished if the subduction channel is much wider (>5 km) below the Mediterranean Sea margin, and much narrower (<1 km) below Tonga.

lower convergence rates and higher rates of delivery to the trench (Clift and Vannucchi, 2004). However, rates of subduction erosion are independent of convergence rate, sediment thickness in the trench, and rates of sediment delivery to the trench as long as the minimum rate of convergence (>60 mm/yr) is exceeded and the maximum values of sediment supply and thickness (<40 km^2/yr; <1 km, respectively) are not. Rates of subduction erosion are also independent of the age of the subducting oceanic crust.

Please cite this article as: Stern, C.R., Subduction erosion: Rates, mechanisms, and its role in arc magmatism and the evolution of the continental crust and mantle, Gondwana Res. (2011), doi:10.1016/j.gr.2011.03.006

Clift and Vannucchi (2004) and Scholl and von Huene (2007, 2009) also conclude that subduction erosion is occurring at margins where accretionary complexes are forming, and furthermore that sediment subduction is occurring at all accretionary margins due to the inefficiency of the accretionary process. Thus there is, in fact, no correlation between the total amount of sediment subducted and convergence rates (Fig. 10B), only a correlation between rates and whether or not the subducted material is sediment delivered to the trench or eroded from the forearc wedge by the subduction process. The implication of this is that subduction channels at slow converging margins, which are characterized by the formation of accretionary complexes (Fig. 10), must be wider than at rapidly converging margins. For example, in order to subduct 100 km^3/km/my of sediment below the Mediterranean ridge in the Aegean Sea at a convergence rate of only 2 cm/yr (MED in Fig. 10; Kopf, 1999; Kopf et al., 2003; Clift and Vannucchi, 2004), the subduction channel must be ~5 km wide. Furthermore, the rates of downward transport of sediment in the subduction channel may be significantly lower than the lower plate velocity (Lohrmann et al., 2006), implying an even wider subduction channel to achieve a given rate of total sediment subduction. Subduction channels have been both calculated and imaged as being 1–7 km in width (von Huene and Scholl, 1991; ANCORP Working Group, 2003; Lohrmann et al., 2006; Scholl and von Huene, 2007, 2009).

This information suggests that subduction erosion is favored by relatively narrow subduction channels, which occurs where high rates of convergence can move a greater total amount of sediment into the mantle (Fig. 10B). Narrower channels may be less smooth than wider channels and thereby enhance the mechanical effect of topographic highs and lows on the subducting plate and thus favors interplate abrasion and basal subduction erosion. Nevertheless, Kukowski and Oncken (2006) attribute increased rates of subduction erosion below central Chile to the widening of the subduction channel caused by the subduction of the Juan Fernández Ridge, thus allowing more rapid transport of sediment and debris in the trench. This may be correct in this specific case because the trench at the locus of subduction of this ridge has a relatively thick, 2.5 km sedimentary infill. The very high rates of subduction erosion (~440 km^3/km/my; Bourgois et al., 1996) associated with the subduction of the Chile Rise also suggest that a relatively wide subduction channel is produced by the subduction of the ridge. However, in general, a narrower rather than a wider subduction channel appears to favor or be associated with subduction erosion.

3.4. Role of subducted material

Cloos and Shreve (1988a, 1988b) modeled aspects of the role of the subduction channel in affecting rates of subduction erosion, and conclude that the capacity of the channel is influenced in part by the physical properties of the subducting material. Lamb and Davis (2003) also suggest that in margins with high sediment supply to the trench, layered turbidite sequences smooth out the top of the subducting plate and provide an abundant source of weak water-rich lubricating material along the plate interface, while in contrast, the chaotic debris cannibalized from the plate toe in erosive margins does not have the same lubricating effect (Fig. 11). Cloos and Shreve (1988a, 1988b) also suggested that low angle subduction enhances rates of subduction erosion relative to high angle subduction.

3.5. Summary

In summary, at margins with rapid convergence rates and low rates sediment supply to the trench, the subduction channel is relatively narrow and thus less smooth, and the chaotic sedimentary debris transported into the mantle in the channel does not lubricate the channel to the same extent as at margins with high rates of sediment supply and thick turbidite layers in the trench. Together the combination of these two effects results in higher rates of subduction erosion than at accretionary boundaries. Subduction of buoyant features weakens the fore-arc wedge, greatly enhancing rates of subduction erosion.

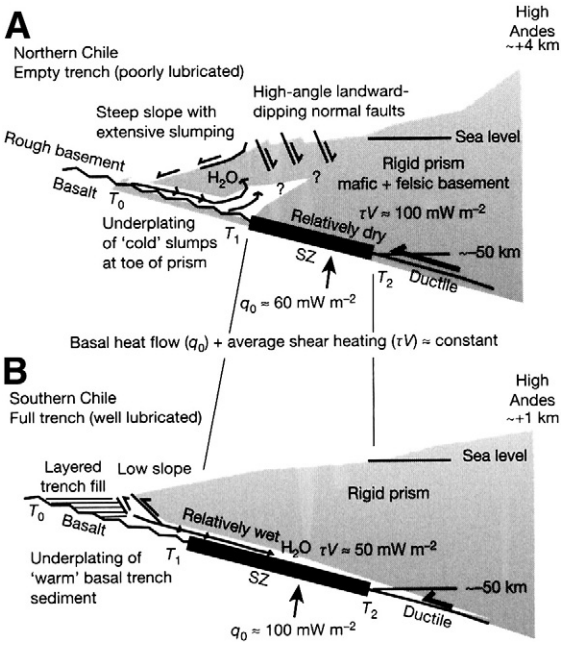

Fig. 11. Cartoon, from Lamb and Davis (2003), illustrating how presence of absence of significant trench fill affects the process of subduction. (A) Subduction erosion along a sediment starved trench, such as in northern Chile, drags chaotic and coarse debris into the subduction zone. (B) A trench filled with well stratified fine-grained sediment, such as in southern Chile, may result in a well lubricated and smooth subduction zone because the wet sediment may form a weak detachment surface extending far down the plate interface.

4. Recycling of subducted crust

Material removed from the forearc wedge by subduction erosion may be recycled back into the crust by being under-plated below the wedge or incorporated into arc magmas.

4.1. Under-plating below the forearc wedge

In SW Japan, east of the Median Tectonic Line (MTL; Fig. 4), the crust is composed solely of Late Mesozoic to Cenozoic accretionary complexes (ACs) and meta-AC units that are characterized by subhorizontal stacking of multiply fault-bounded units with a very gentle dip angle towards the Eurasian continent (Isozaki et al., 2010). Recent geophysical analyses confirmed that the AC units penetrate far into the continental side of the island, even beyond the surface transect of the MTL (Ito et al., 2009). Thus some significant proportion of subducted sediment and forearc crust has remained within the crust of SW Japan, and has not been subducted deeper into the mantle.

However, it is also clear that in SW Japan under-plating has been associated with uplift and erosion of the overlying crust (Fig. 4). This also occurred in the southwest US during late Cretaceous times (Fig. 5; Grove et al., 2008; Jacobson et al., 2011). In contrast to SW Japan, where the accretionary and meta-accretionary units young towards the trench, the oldest meta-accretionary units occur closer to the coast in the southwest US (Grove et al., 2003, 2008; Jacobson et al., 2011). Grove et al. (2003) proposed that removal of the base of North America by subduction erosion associated with progressive flattening of the angle of subduction caused younger schists to be under-plated at increasingly greater distances inboard, above the hinge at which

Please cite this article as: Stern, C.R., Subduction erosion: Rates, mechanisms, and its role in arc magmatism and the evolution of the continental crust and mantle, Gondwana Res. (2011), doi:10.1016/j.gr.2011.03.006

the subducting plate descended towards the mantle (Fig. 5). As the flattening slab continued to erode inboard, the locus of under-plating migrated in the same direction, leading to progressively younger packets of accreted material away from the trench, as well as the uplift and erosional denudation of the overlying crust (Fig. 5).

Clift and Hartley (2007) also conclude that under-plating below the onshore portion of the forearc wedge in southern Peru and northern Chile, of either subducted sediment or basement rocks stripped from under the trenchward offshore parts of the forearc by basal subduction erosion, has resulted in uplift of previously subsiding onshore basins. Their isostatic volume estimates suggest that as much as 85% of subducted material was under-plated under the onshore forearc since 330 ka. However, trench retreat combined with onshore uplift has resulted in a steepening of the forearc taper. Because the margin cannot continue to steepen and shorten in this fashion indefinitely, this style of margin evolution cannot be steady-state, but will at some point likely return to the conditions of faster tectonic erosion and coastal retreat, with steady-state margin geometry, that has characterized this part of the central Andes over the last 150 Ma.

Thus it appears that under-plating leads to more rapid forearc erosion, and over the long term cannot accommodate a large proportion of subducted crust without leading to more rapid rates of subduction erosion. von Huene and Scholl (1991) and Scholl and von Huene (2007, 2009) also note that, globally, exposed tracks of high-pressure crustal under-plates are volumetrically small compared to the volume of continental material missing due to subduction erosion. They conclude that, except where flat-slab subduction has replaced the lower crust with an under-plate of subducted sediment far inboard of the coast such as in the SW US (Fig. 5; Grove et al., 2003, 2008; Jacobson et al., 2011), the bulk of under-plated material is only temporarily stored beneath the coastal area of the forearc wedge, and that as subduction erosion progressively narrows and thins a margin's inner rock prism, the coastal under-plate is flushed into the mantle.

4.2. Incorporation into arc magmas

Geochemical evidence abounds for the incorporation of subducted sediments into arc magmas (Kay et al., 1978; Armstrong, 1981, 1991; Woodhead and Fraser, 1985; Tera et al., 1986; White and Dupré, 1986; Sigmarsson et al., 1990, 1998, 2002; Plank and Langmuir, 1993, 1998; Elliott et al., 1997; Pearce et al., 1999), as originally proposed by Coats (1962). Some of this evidence, including Be and Pb isotopic data, implies that this is a pelagic sediment component (Barreiro, 1984; Morris et al., 1990; Sigmarsson et al., 1990; Macfarlane, 1999; Hickey-Vargas et al., 2002). However, as reviewed above, continental crust is also being subducted, both due to subduction erosion and in the form of terrigenous sediments, and at many if not most margins in much greater proportions than pelagic sediments. The evidence for the recycling of this subducted continental crust, and specifically crust subducted due to subduction erosion, is well documented, as reviewed below, in detailed studies of magma petrogenesis in a number of arcs.

Components from subducted oceanic crust, including fresh and altered mid-ocean ridge basalts (MORB), pelagic and terrigenous sediments and material derived from the forearc crystalline wedge by subduction erosion, may contribute to the formation of arc magmas by 1) being added to the mantle source region of arc basalts (IAB) as melts, or, more probably, as soluble constituents of aqueous fluids due to the dehydration of the subducted slab as a result of pressure induced break-down of hydrous phases; and/or 2) melting of the subducted crust and sediment resulting in adakitic magmas that either erupt directly to the surface, mix with other slab-derived or mantle melts, and/or interact with mantle peridotite as they rise to the surface. In arcs where mantle-derived basalts comprise a significant proportion of the erupted arc magmas, aqueous fluid transfer of subducted crust into the overlying mantle source of these

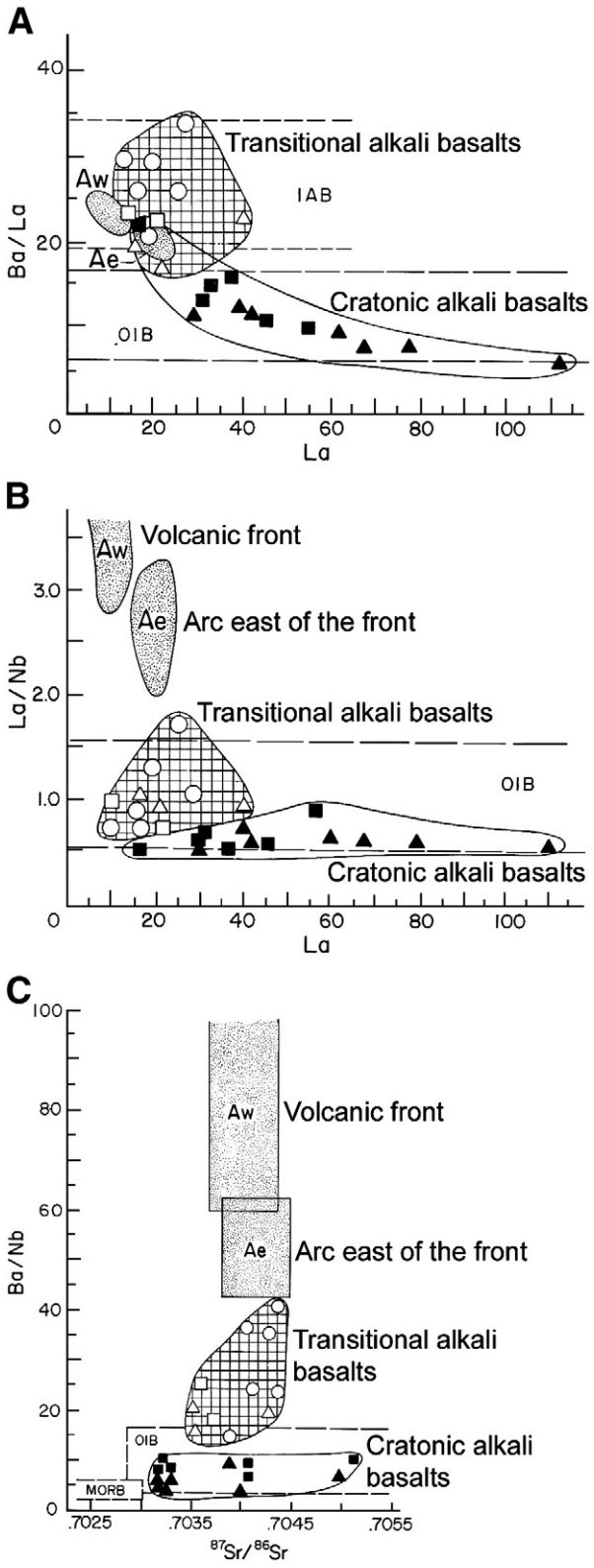

Fig. 12. (A) Ba/La versus La content; (B) La/Nb versus La content; and (C) Ba/Nb versus $^{87}Sr/^{86}Sr$, for samples from along the volcanic front (Aw) of the Andean central SVZ (Fig. 6), centers east of the front (Ae), and back-arc alkali basalts in areas of Cenozoic arc volcanism (transitional alkali basalts) and cratonic regions that have not experienced Cenozoic arc volcanism (cratonic alkali basalts; Stern et al., 1990). The figure illustrates the higher Ba/La, La/Nb and Ba/Nb ratios, and La contents, from west to east across the Andean SVZ arc and into the back-arc region, interpreted to result from decreasing influx of slab-derived fluids into the subarc asthenospheric mantle wedge, and, as a consequence, decreasing degree of partial mantle melting across the arc.

Please cite this article as: Stern, C.R., Subduction erosion: Rates, mechanisms, and its role in arc magmatism and the evolution of the continental crust and mantle, Gondwana Res. (2011), doi:10.1016/j.gr.2011.03.006

IAB is suggested by their high ratios, compared to oceanic island basalts (OIB), of large-ion-lithophile-elements (LILE) to rare-earth-elements (REE; for example Ba/La; Fig. 12A), REE to high-field-strength-elements (HFSE; for example La/Nb; Fig. 12B), and very high ratios of LILE to HFSE (for example Ba/Nb; Fig. 12C), which reflect the fact that LILE are more soluble than REE, and REE more soluble than HFSE, and therefore relatively enriched in slab-derived fluids (Hickey et al., 1986; Hickey-Vargas et al., 1989; Stern et al., 1990). Also, excess ^{226}Ra over ^{230}Th and ^{238}U over ^{230}Th both imply addition of slab-derived aqueous fluids rather than melts to the mantle magma source (Sigmarsson et al., 1998, 2002). Furthermore, Sr, Nd and $\delta^{18}O$ isotopic values often indicate only a small difference between IAB and OIB, which implies that the mass of components derived from the subducted slab must be small relative to the mass of the mantle source of these basalts (Fig. 12C; Hickey et al., 1986; Hickey-Vargas et al., 1989; Stern et al., 1990; Clift et al., 2009a). In contrast, in arcs or arc segments where basalts are absent or less significant, and adakitic andesites comprise a significant proportion of the erupted arc magmas, melting of the subducted slab, including sediment, has been suggested as the source of these adakites (Defant and Drummond, 1990; Defant et al., 1991; Sen and Dunn, 1994; Yogodzinski et al., 1994; Stern and Kilian, 1996; Sigmarsson et al., 1998; Shimoda et al., 1998; Tatsumi, 2001; Kilian and Stern, 2002; Bindeman et al., 2005), or the chemically similar tonalite–trondjhemite–granodiorite (TTG) plutonic rock suites (Martin, 1986; Drummond and Defant, 1990; Rapp et al., 1991; Rapp and Watson, 1995). These two cases are considered separately below.

4.2.1. Mantle-source-region contamination by slab-derived fluids

Plank and Langmuir (1993, 1998) present a model constraining the global input of subducted trench sediments, including both pelagic and terrigenous sediments, into arc magmas. Clift et al. (2009a) have modified their model to account for the estimated proportion of crust derived from the forearc wedge by subduction erosion (1.35 AU) that is also being subducted along with trench sediments (1.65 AU). The model of Clift et al. (2009a) is based on mass balance using the Nd isotope character, expressed as ε_{Nd}, and Nd concentrations for both the subducting trench sediments and forearc crust at different subduction zones, as well as the presumed composition of melts from the subarc mantle, in order to quantify the degree of crustal recycling associated with magma genesis at convergent plate boundaries. They consider a value of $\varepsilon_{Nd} \approx 10$ to be appropriate for the unmodified subarc mantle, based on the composition of mid ocean ridge basalts (MORB; White and Hofman, 1982), although this value is higher than typical for the most primitive arc basalts. They derive an average value of ε_{Nd} for the magmatic output at each arc using the published data sets of GEOROC (http://georoc.mpch-mainz.gwdg.de/georoc/), and demonstrate that arc magmatic rocks are systematically displaced to lower values of ε_{Nd} than MORB-source mantle due to the input of subducted sediment and forearc wedge crust into the subarc mantle. They calculate the Nd isotope compositions of the continental material being subducted by mixing the trench sediment and the forearc end members in the proportions determined by Clift and Vannucchi (2004). Having established the end member compositions, they un-mix the Nd composition of the magmatic output to determine the influence of subducted continental crust on petrogenesis in each arc. The results of their analysis (Fig. 13) suggest that at a global level only around 25% of the crustal Nd passing below the marine portion of the forearcs is recycled directly into arc magmatic rocks. Fig. 14 illustrates in a triangular diagram the relative proportions between mantle, subducted sediment and subducted forearc crust that Clift et al. (2009a) determined for arc magmas along the different convergent plate boundaries for which the total sedimentary input is illustrated in Fig. 13.

The mass balance calculations of Clift et al. (2009a) are based exclusively on Nd, which they consider is a water-immobile element, but which may be transported with other light-rare-earth-elements in slab-derived fluid preferentially to more insoluble elements high-field-strength elements (Fig. 12B). Therefore, the percent of Nd recycled may be larger than the actual total crustal material recycled. Clift et al. (2009a) further caution that even the low degree of crustal recycling they calculate must be considered a maximum, because they do not correct for the effects of crustal assimilation into the melts on their way to the surface in continental arcs. They conclude that overall, only 20% of subducted crust returns to the crust though arc magmatism and 80% is subducted into the deeper mantle.

Stern et al. (2011), in correlating temporal changes in magma chemistry and rates of subduction erosion in the Andes of central Chile, avoid the problems associated with crustal assimilation by focusing only on subarc mantle-derived olivine basalts. In the Andes of central Chile, at latitude 34°S (Fig. 6), just south of the locus of subduction of the Juan Fernández Ridge, the Nd, Sr and Pb isotopic composition of olivine-bearing basalts, and by implication their mantle source region, have changed significantly through time, between the late Oligocene and the present (Figs. 15 and 16; Stern and Skewes, 1995; Kay et al., 2005; Stern et al., 2010, 2011). Late

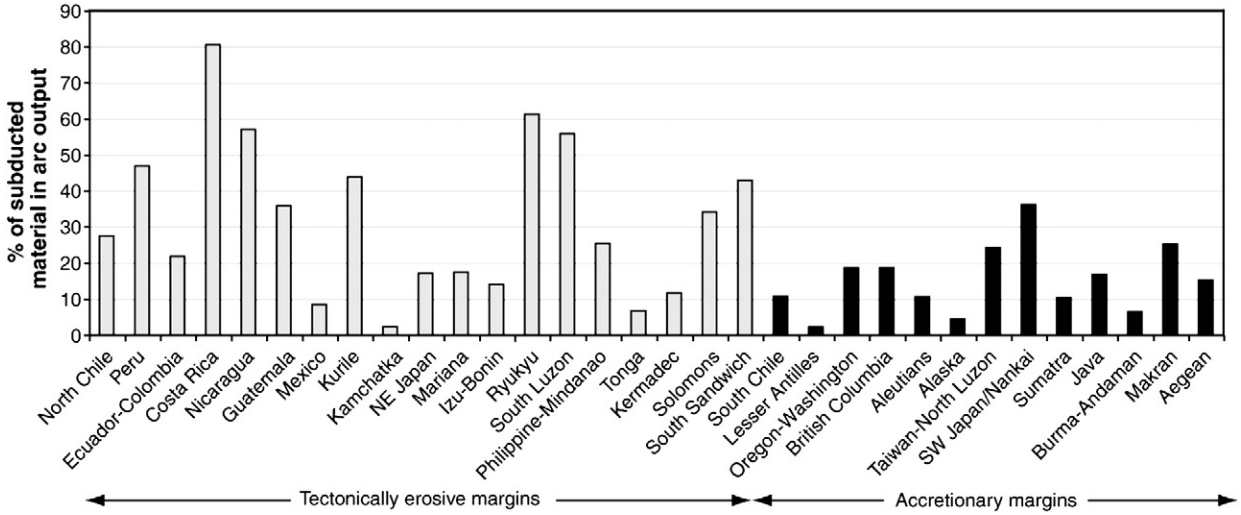

Fig. 13. Bar graph, from Clift et al. (2009a), showing the long-term average proportion of the crustal material subducted at the major subduction zones that is recycled back into the magmatic products of the associated arc complex. Shaded bars are for margins with active subdcution erosion, so that some portion of the crustal material is forearc basement (Fig. 14), while solid bars are for accreting margins.

Please cite this article as: Stern, C.R., Subduction erosion: Rates, mechanisms, and its role in arc magmatism and the evolution of the continental crust and mantle, Gondwana Res. (2011), doi:10.1016/j.gr.2011.03.006

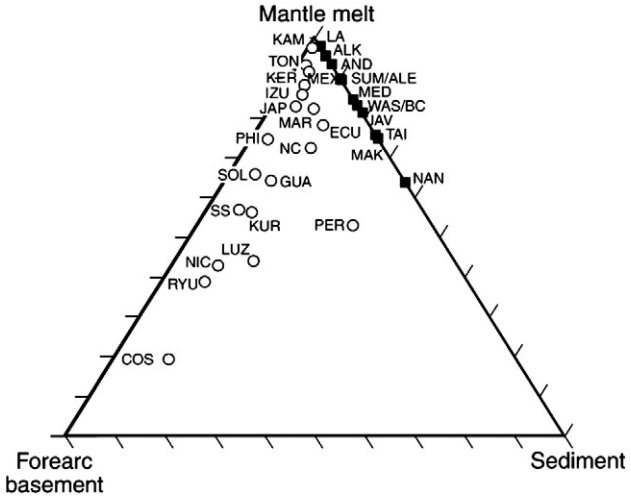

Fig. 14. Triangular diagram, from Clift et al. (2009a), showing the estimated contributions from new mantle wedge melt, recycled trench sediment and eroded forearc crust to the net magmatic output of the major subduction systems. Black squares show accretionary margins and open circle represents tectonically erosive margins.

Oligocene to early Miocene (>15 Ma) Abanico or Coya-Machalí Formation volcanic and plutonic rocks in the region have relatively high $\varepsilon_{Nd} = +3.8$ to $+6.2$ and low $^{87}Sr/^{86}Sr = 0.7033$ to 0.7039 and $^{206}Pb/^{204}Pb = 18.45$ to 18.57, while middle to late Miocene (6.5–13.9 Ma) El Teniente Volcanic and Plutonic Complex igneous rocks have lower $\varepsilon_{Nd} = +1.9$ to $+3.8$ and higher $^{87}Sr/^{86}Sr = 0.7039$ to 0.7041 and $^{206}Pb/^{204}Pb = 18.56$ to18.59, and Pliocene (3.9–2.9 Ma) olivine lamprophyre dikes, as well as younger (2.3 Ma to Recent) olivine-bearing basaltic-andesites, have even lower $\varepsilon_{Nd} = +1.2$ to -1.1 and higher $^{87}Sr/^{86}Sr = 0.7041$ to 0.7049 and $^{206}Pb/^{204}Pb = 18.60$ to 18.68. These igneous rocks were all emplaced in a small area and thus generated in a common vertical column of mantle and crust. At each stage, the isotopic composition of andesites and dacites associated with basalts of the same age has similar isotopic compositions to the associated basalts (Fig. 15B), which precludes contamination by isotopically heterogeneous Paleozoic and Mesozoic continental crust during evolution of these intermediate and silicic rocks from the mantle-derived mafic magmas.

The late Oligocene to Recent isotopic evolution of the mantle source of the mafic magmas in central Chile may be explained by an increase from 1% to 6% in the extent of mantle source region contamination by subducted components, including continental crust tectonically eroded off the continental margin (Fig. 17). Increasing $^{206}Pb/^{204}Pb$ is also consistent with increasing component of subducted crust and sediment in the source of these arc magmas (Fig. 16; Stern et al., 2011). The 1 to 6% of recycled Nd and Sr in the arc magmas of different ages erupted in central Chile were calculated based on a subarc mantle with initially $\varepsilon_{Nd} = +7$, rather than the value of $\varepsilon_{Nd} = +10$ employed for the mantle by Clift et al. (2009a), and these percentages of subducted crust involved in the generation of the youngest rocks are thus lower than that calculated by Clift et al. (2009a).

These temporal changes in magma chemistry correlate with increasing rates of subduction erosion along this area of the southern Andean margin. Kay et al. (2005) estimate that 35 km of the fore-arc wedge was removed by subduction erosion at this latitude (34°S) between 16 and 19 Ma, and another 50 km of the fore-arc was removed from 7 to 3 Ma (Fig. 6). Stern (1991, 2004), Stern and Skewes (1995) and Stern et al. (2011) suggest that increased rates of subduction erosion at this latitude during the late Miocene were associated with the southward migration of the locus of subduction of the Juan Fernández Ridge. As discussed above, Kukowski and Oncken (2006) calculate a long-term rate of subduction erosion of 25–35 km^3/km/my for central Chile from 33 to 40°S, while since 9 Ma the average rate for the region between 33 and 36°S was 115 km^3/km/my, and the rate of subduction erosion where the ridge is currently being subducted is 96–128 km^3/km/my (Laursen et al., 2002; Kukowski and Oncken, 2006). Stern and Skewes (1995) demonstrate that the isotopic changes that have occurred between the late Miocene and the Pliocene at latitude 34°S, also occurred progressively earlier further to the north, at 8 Ma at 33°S and at 12 Ma at 32°S. They attribute this to the southward migration of the locus of subduction of the Juan Fernández Ridge (Yáñez et al., 2001, 2002), which also caused a decrease in subduction angle and eastward migration of the arc. Overall the data suggest a close temporal correlation between the enhanced rates of subduction erosion associated with the subduction of the Juan Fernández Ridge, and increased crustal components in the mantle source of mafic igneous rocks formed in central Chile.

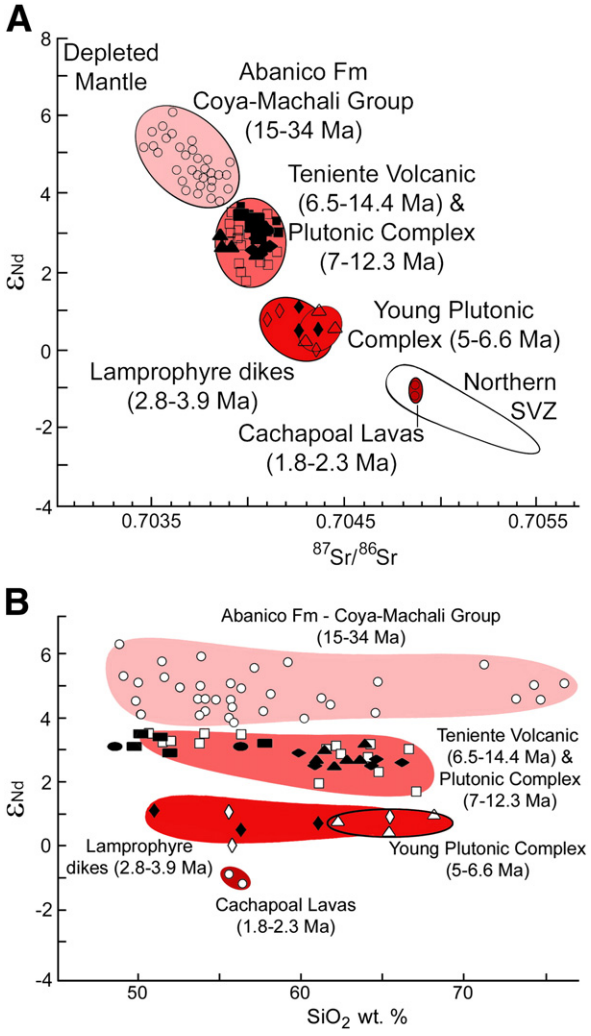

Fig. 15. (A) $^{87}Sr/^{86}Sr$ versus ε_{Nd} for samples of different ages from the vicinity of El Teniente Cu-deposit at 34°S (Fig. 6) in the Andes of central Chile (Stern and Skewes, 1995; Kay et al., 2005; Stern et al., 2010, 2011). The figure illustrates the progressive temporal increase in $^{87}Sr/^{86}Sr$ and decrease in ε_{Nd} from the early Miocene to the Pliocene for igneous rocks at the latitude of El Teniente. Fig. 6 shows the outcrop of the Late Oligocene to Early Miocene Abanico Formation (pink) and the Middle to Late Miocene Teniente Volcanic and Plutonic Complexes (light red), but the Late Miocene to Pliocene Younger Plutonic Complex and Lamprophyre Dikes (darker red) and the Pliocene Cachapoal lavas (darkest red), both of which occur within the area of the older Miocene rocks, are too small in volume to appear on this map. (B) SiO_2 versus ε_{Nd} for the same samples, illustrating both their progressive temporal decrease in ε_{Nd} from the early Miocene to the Pliocene, and the independence during each specific time interval of isotopic composition and SiO_2.

Please cite this article as: Stern, C.R., Subduction erosion: Rates, mechanisms, and its role in arc magmatism and the evolution of the continental crust and mantle, Gondwana Res. (2011), doi:10.1016/j.gr.2011.03.006

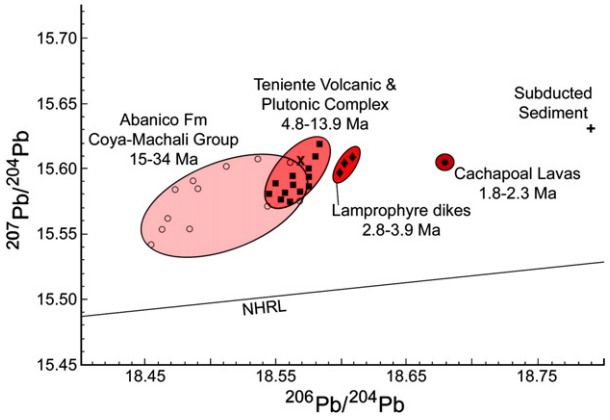

Fig. 16. $^{206}Pb/^{204}Pb$ versus $^{207}Pb/^{204}Pb$ for samples from the vicinity of El Teniente Cu-deposit at 34°S in the Andes of central Chile (Stern et al., 2011), and the Pb isotopic composition of a model subducted sediment (+), including subducted continental crust, as calculated by Macfarlane (1999).The data show a temporal trend of $^{206}Pb/^{204}Pb$ towards this value.

As pointed out by Stern and Skewes (1995), Kay et al. (2005) and Stern et al. (2011), the temporal changes in magma isotope chemistry observed at 34°S between the late Oligocene and present are similar to changes observed from south-to-north along the active Andean SVZ arc between 36 and 33°S (Fig. 6; Futa and Stern, 1988; Hildreth and Moorbath, 1988; Stern, 1991, 2004; Stern et al., 2007). Hildreth and Moorbath (1988) attributed this to increasing crustal thickness to the north. However, as discussed above and in Stern et al. (2011), these changes are observed in the most mafic olivine-bearing rocks erupted in this sector of the Andean arc, and the amount of crustal assimilation required to produce these changes is greater than allowable to maintain the mafic character of these rocks, implying that they are produced by isotopic changes in their mantle source. Northward from 36°S the rate of subduction erosion also increases, from <35 km^3/km/my to >120 km^3/km/my at 33°S where the Juan Fernández Ridge is being subducted. The close spatial correlation between the northward changes in this rate and the isotopic composition of the most mafic magmas erupted northward in this segment of the Andean arc is consistent with the observed spatial changes in isotopic compositions of Andean magmas having been produced by the northward increase in the rates of subduction erosion and mantle source region contamination by subducted forearc crust (Stern, 1991, 2004; Stern and Skewes, 1995; Kay et al., 2005; Stern et al., 2007, 2011).

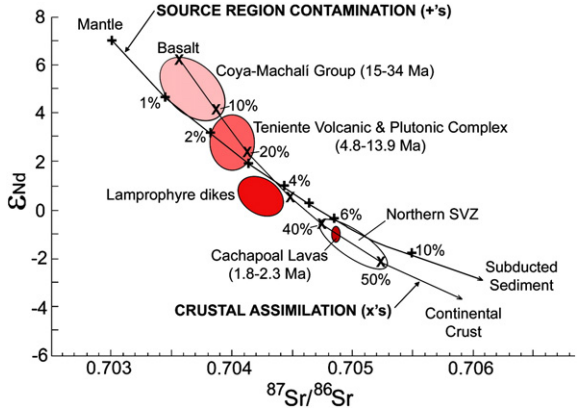

Fig. 17. Sr versus Nd isotopic values, from Fig. 15, of the various groups of igneous rocks of different ages across a transect of the Andes at the latitude of El Teniente Cu-deposit at 34°S in the Andes of central Chile. The figure illustrates both a source region contamination model of primitive mantle (36 ppm Sr with $^{87}Sr/^{86}Sr = 0.703$; 1.8 ppm Nd with $\varepsilon_{Nd} = +7$) mixed with various proportions of subducted sediment (380 ppm Sr with $^{87}Sr/^{86}Sr = 0.70763$; 42.3 ppm Nd with $\varepsilon_{Nd} = -5.1$; Macfarlane, 1999), and also an assimilation model, taken from Kay et al. (2005), for a Coya-Machalí basalt (450 ppm Sr with $^{87}Sr/^{86}Sr = 0.7035$; 9 ppm Nd with $\varepsilon_{Nd} = +6$) assimilating various proportions of Paleozoic–Triassic Andean granite basement (350 ppm Sr with $^{87}Sr/^{86}Sr = 0.7075$; 20 ppm Nd with $\varepsilon_{Nd} = -6$). Both models reproduce the isotopic compositions of the progressively younger rocks in the transect, but the latter model requires assimilation of unacceptably high proportions of granite crust and is inconsistent with the generation of low SiO_2 primitive olivine-bearing mafic rocks in each age group, as well as the progressively higher Sr content of the younger rocks (Stern et al., 2011).

In central Chile, as subduction angle decreased above the modern zone of flat-slab subduction (28–33°S) during the Miocene, igneous rocks were formed with progressively higher $^{87}Sr/^{86}Sr$ and lower ε_{Nd} (Kay et al., 1991). Kay et al. (1991) suggest that the observed isotopic changes were similar to those observed along strike from south-to-north at the northern end of the Anden SVZ arc between 36 and 33°S. They proposed that these isotopic changes could have resulted from increased mantle-source region contamination associated with an increasing contribution of subducted forearc crust due to the increasingly shallow dip of the slab thought time. As discussed above, Stern (1991) calculated an enhanced subduction erosion rate of 84 km^3/km/my in this region over the last 15 my, and attributed this to both decreasing subduction angle beginning in the middle Miocene and the subduction of the Juan Fernández Ridge below this region.

In the central Andes of northern Chile, below which the crust is very thick (>70 km), Andean volcanic rocks have generally low $\varepsilon_{Nd} \leq 2$ and high $^{87}Sr/^{86}Sr$ >0.7055 due to incorporation of crustal components (Stern, 2004; Stern et al., 2007). Here the Miocene to recent arc has migrated east to its current position due to progressive subduction erosion along the trench (Rutland, 1971; Ziegler et al., 1981; Stern, 1991; von Huene and Scholl, 1991). Rogers and Hawkesworth (1989) demonstrated that as the arc migrated eastward, ε_{Nd} decreased and $^{87}Sr/^{86}Sr$ increased to their present values, and that increasing $^{87}Sr/^{86}Sr$ was associated with increasing Sr concentrations in magmatic rocks. This trend is inconsistent with increased shallow crustal assimilation, which results in decreasing Sr concentrations with increasing $^{87}Sr/^{86}Sr$. They therefore attributed this trend, not to the increased crustal thickness below the active arc, but instead to increased mobilization of older, late Proterozoic subcontinental mantle lithosphere. Stern (1990, 1991) argued instead that this same trend could also be produced by increased mantle source region contamination as a result of increased rates of subduction erosion as arid conditions reduced the sediment supply to the trench in the Miocene, and the Juan Fernández Ridge was subducted below northern Chile beginning at 23 Ma (Yáñez et al., 2001, 2002; Kay and Coira, 2009). This would require source region contamination by approximately 10% subducted crust to produce the isotopic composition of the most mafic magmas erupted in the central Andes of northern Chile (Fig. 17; Stern, 1990, 1991, 2004; Macfarlane, 1999; Stern et al., 2007). Clift et al. (2009a) calculate an even higher 27% of subducted sediment in arc magmas in northern Chile (Fig. 13), again in part because they begin with a more primitive mantle $\varepsilon_{Nd} = +10$ and ignore the effects of intracrustal contamination. In either case, the significant point is that in the extremely arid area of northern Chile, where the rate of sediment supply to the trench is very low, the bulk of subducted material is derived from forearc subduction erosion, confirming its participation in arc magmas generated in this segment of the Andes.

Another arc segment for which the composition of fore-arc materials and both the spatial variations and timing of isotopic changes in the composition of arc magmas suggest mantle source region contamination resulting from subduction erosion is the central American country of Costa Rica (Clift et al., 2005, 2009b). On the basis of the 3–5 km subsidence of outer forearc basal sediments and the presence of a margin-wide seismic reflector marking the base of slope sediment along the Nicoya shelf, Meschede et al. (1999), Ranero and von Huene (2000), and Vannucchi et al. (2001, 2003) estimated long-term subduction erosion rates of 34–36 km^3/km/my over the last 17 Ma. Here subduction erosion transports into the mantle a chemically distinctive forearc

Please cite this article as: Stern, C.R., Subduction erosion: Rates, mechanisms, and its role in arc magmatism and the evolution of the continental crust and mantle, Gondwana Res. (2011), doi:10.1016/j.gr.2011.03.006

basement component derived from the Nicoya and other ophiolite complexes (Meschede et al., 1999; Ranero and von Huene, 2000; Vannucchi et al., 2001, 2003; Goss and Kay, 2006). Clift and Vannucchi (2004) estimated that the total proportions of eroded forearc and incoming sediments subducted below Costa Rica in the last 6 Ma included 86% subducted forearc material. Clift et al. (2005) employed Li and Nd isotopes of unaltered volcanic tephra younger than 2.5 Ma to quantify the influence of sediment subduction and tectonic erosion on Pliocene arc petrogenesis in Costa Rica. They determined that the chemistry of these tephra requires both a forearc Nicoya Ophiolite Complex and trench sediment component subducted into their mantle source region (Fig. 18A). Furthermore they identify a unique Nd isotopic chemistry for a 1.45 Ma tephra derived from the Arenal volcano (Fig. 18B). They interpret the temporal patterns of isotope evolution to reflect collision of a seamount with the trench before 1.45 Ma, driving subduction of a sediment wedge formed there, and subsequently increasing erosion and subduction of forearc materials. Goss and Kay (2006) also documented a role for subduction erosion in the genesis of Pliocene adakites in Costa Rica and Panama, discussed in more detail below.

Spatial and temporal correlations have also been made between increased rates of subduction erosion and arc magma chemistry in Japan. Here Takagi (2004) correlated the formation of a pulse of late Cretaceous reduced ilmenite series granites, characterized by relatively low initial ε_{Nd} and high $^{87}Sr/^{86}Sr$ and $\delta^{18}O$ compared to magnetite series granites, with a pulse of relatively high convergence rates (>70 to 200 mm/yr). This caused increased subduction erosion and mixing of components derived from subducted sediments into the mantle source of the granites. Takagi (2004) calculates 15% subducted crustal material incorporated in the source of the ilmenite series granites.

4.2.2. Melting of subducted crust

In some arcs adakitic andesites occur along with basalts, and in some cases they form a significant proportion of the erupted arc magmas (Kay, 1978; Myers et al., 1986; Futa and Stern, 1988; Defant and Drummond, 1990; Yogodzinski et al., 1994; Stern and Kilian, 1996). Adakites are high-Mg andesites characterized by distinctively high La/Yb and Sr/Y, suggesting garnet in their source. In arcs below which the crust is too thin (<40 km) to stabilize garnet in the lower arc crust, adakites have been attributed to melting of subducted oceanic crust, including in some cases sediments. Experimental work has demonstrated that melting of basalt metamorphosed at high pressures to garnet–amphibolite or eclogites produces andesitic melts (Stern, 1974; Rapp et al., 1991; Sen and Dunn, 1994; Rapp and Watson, 1995), and also that subducted sediments melt at lower temperatures than basalts (Stern and Wyllie, 1973; Nichols et al., 1994, 1996; Tatsumi, 2001).

Globally, adakites are less common than basalts in active arcs, but significantly their formation often reflects transient events of accelerated rates of subduction erosion associated with either changes in subduction geometry and/or subduction of buoyant feature such as oceanic ridges or seamounts (Gutscher et al., 2000). For instance, a period of Aleutian forearc subduction erosion at the time of adakite formation (~12 Ma) is indicated by the coincident 30 km northward jump of the magmatic line (Fig. 19). Kay (2006) has reinterpreted the formation of the type adakite from Adak Island in the Aleutians (Kay, 1978) as having resulted from melting, at high pressure, of mafic (MORB) crust plucked from the forearc basement (Kay et al., 1986) as a result of subduction erosion associated with the relocation of the magmatic front into the former backarc.

Crustal materials, subducted due to subduction erosion, are also involved in a transient event of adakite magma genesis above the Chile Rise-Trench triple junction in the southernmost Andes (Figs. 7 and 8). Bourgois et al. (1996) characterize the 3.3–5.1 Ma Caber Raper pluton on Peninsula Taitao as a Na-rich trondhjemitic-tonalite, with low Yb, implying garnet and hornblende in the magmatic source, which they consider to be metamorphosed subducted oceanic crust. The low $\varepsilon_{Nd} = +1.5$ and high $^{87}Sr/^{86}Sr = 0.7045$ suggest participation of 10–20% subducted continental material in the melt (Guivel et al., 1999; Lagabrielle et al., 2000). This pluton formed as the segment of the Chile Rise between the Taitao and Tres Montes fractures zones was being subducted (Fig. 7), and the participation of subducted continental crust in the genesis of this pluton is consistent with the high rates of subduction erosion associated with ridge subduction. Younger (70 ka to 2 Ma) high and low silica dacites, dredged from

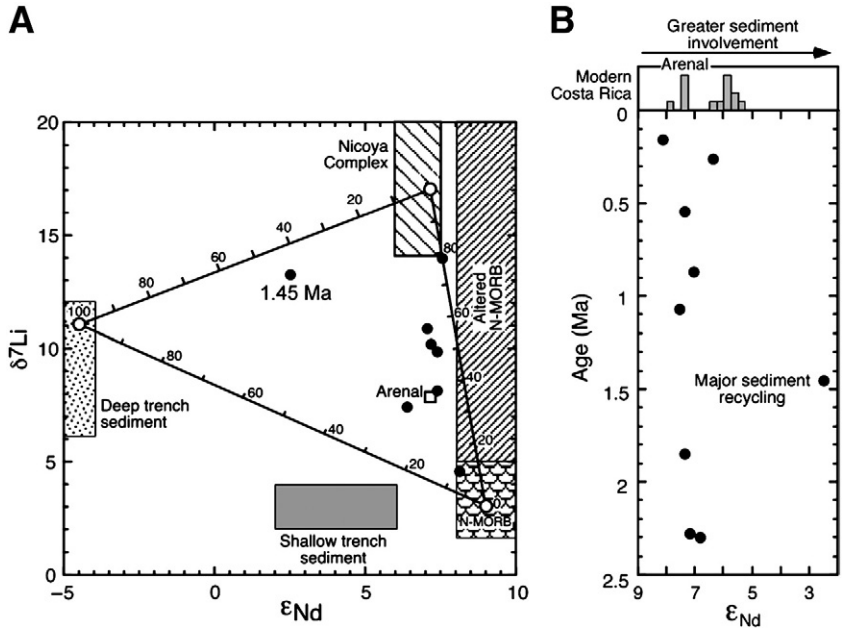

Fig. 18. (A) Plot of ε_{Nd} and δ^7Li, from Clift et al. (2005, 2009b), showing that although the majority of tephra glasses from Costa Rica volcanoes could be explained by mixing recycled MORB crust and subducted sediments, an additional, probably forearc sediment component is required. (B) Diagrams showing the evolving Nd isotopic composition of Costa Rican tephras since 2.5 Ma. Histogram of ε_{Nd} values for modern Costa Rica is from GEOROC. Diagram shows the strong temporal variability in the degree of sediment and forearc crustal recycling, probably linked to seamount collision.

Please cite this article as: Stern, C.R., Subduction erosion: Rates, mechanisms, and its role in arc magmatism and the evolution of the continental crust and mantle, Gondwana Res. (2011), doi:10.1016/j.gr.2011.03.006

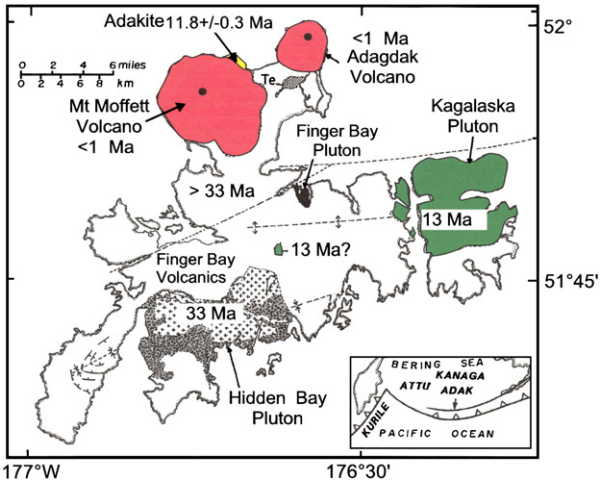

Fig. 19. Map of Adak Island, Alaska, from Kay et al. (1986) and Kay (2006), illustrating the type locality for adakite (Kay, 1978), which formed at ~12 Ma as a result of a period of enhanced subduction erosion of mafic (MORB) arc basement associated with changes in subduction geometry that lead to the migration of the volcanic front 40 km to the north.

both the Taitao ridge as well as the inner wall of the Chile trench, are associated with the currently active triple junction below which the segment of the Chile Rise between the Taitao and Darwin fracture zones is being subducted (Fig. 8). The low silica dacites have relatively high Sr/Y and low Yb similar to other adakites worldwide, and are also formed by melting of a subducted MORB + sediment source at depths of 25–45 km (Guivel et al., 2003). The high silica dacites formed at shallower depths of <25 km where plagioclase and amphibole are stable, from a source that consists of a mixture of 75% subducted basalt and 25% subducted sediment (Guivel et al., 2003).

In southern Costa Rica and central Panama, ~120 km of apparent arc migration since the Eocene has been attributed to subduction erosion, but accelerated subduction erosion along the Costa Rican margin during the last 5–6 Ma is supported by sediment drilling records that indicate a dramatic landward shift in the coastline coincident with a 40 to 50 km NE migration of the arc volcanic front (Meschede et al., 1999). The appearance of adakitic magmas, with steep rare earth element (REE) patterns, at ~4 Ma coincides with the collision of the Cocos Ridge and the inception of slab shallowing along the margin in southern Costa Rica and Panama (Fig. 20; Defant et al., 1991; Goss and Kay, 2006). Partial melting of crust removed from the base of the forearc and subjected to high-pressure metamorphism in the subduction channel provides an explanation for the steep adakitic REE patterns in these arc lavas, because crustal thicknesses below this part of the central American arc are insufficient (<40 km) to permit garnet-bearing lower crustal residues. Distinctly higher $^{206}Pb/^{204}Pb$ and $^{208}Pb/^{204}Pb$ ratios in these adakitic lavas than in older Miocene lavas suggest that components enriched in radiogenic Pb also entered the mantle magma source at ~4 Ma. The incorporation into the mantle wedge by subduction erosion of Cretaceous and early Tertiary ophiolites in the forearc (Fig. 20), whose origins have been linked to the Galapagos hot spot, can explain the along-arc spatial and temporal patterns of Pb-isotopic ratios in southern Central American arc lavas (Goss and Kay, 2006). Clift et al. (2009a) calculate that 70% of the subducted forearc crust is recycled into Costa Rican arc magmas, but isotopic modeling suggests that only ~50–55% of the Pb recycled to the Costa Rican crust via subduction zone volcanism during the last 6 Ma can be explained by Pb added to the mantle wedge from subducted forearc ophiolites (Goss and Kay, 2006).

Shimoda et al. (1998) and Tatsumi (2001) concluded that the high-Mg andesite magmas in the Miocene Setouchi volcanic belt, southwest Japan (Fig. 21), are likely to have formed via partial melting of subducting trench sediments. The isotopic signatures of these high-Mg andesites overlap with those of terrigenous trench-fill sediments derived from the Japan forearc (Fig. 4). The production of silicic melts from the sediments was followed by the reaction of such melts with overlying mantle peridotites, resulting in the dissolution of olivine and clinopyroxene and precipitation of orthopyroxene to produce a high-Mg andesite. The total weight percent of sediment involved in the final magma is estimated to be approximately 60%.

Large volume Phanerozoic plutonic belts, with geochemical characteristics such as high Na, Sr, and La/Yb and low Yb and Y similar to adakites and Archean tonalite–trondhjemite–granodiorite (TTG) granitoids, include the Cordillera Blanca batholiths in Peru (Atherton and Petford, 1993, 1996; Petford and Atherton, 1996), the Separation Point suite of the Median batholiths in New Zealand (Tulloch and Kimbrough, 2003), and the La Posta suite along the eastern edge of the Peninsula Range batholith in southern California and Baja, Mexico (Gromet and Silver, 1987; Tulloch and Kimbrough, 2003; Kimbrough and Grove, 2006; Grove et al., 2008). All these formed after and inboard, towards the continental interior, of older

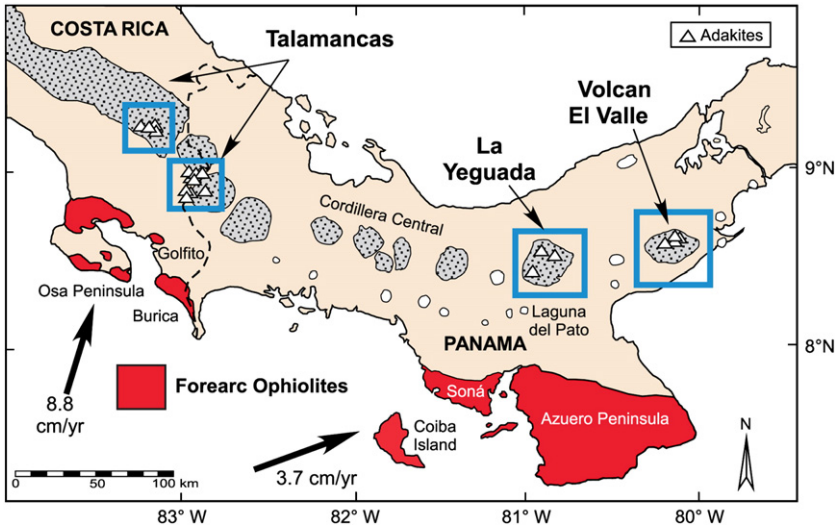

Fig. 20. Map of southeastern Costa Rica and western Panama from Defant et al. (1991) and Goss and Kay (2006). Geographic exposures of forearc ophiolite complexes (Osa, Burica, Golfito, Coiba Island, Soná, and Azuero) are shown by solid red fields. Stippled gray fields represent major volcanic centers of the Quaternary volcanic arc of Panama and Cordillera de Talamanca. Smaller cones and domes are shown in white. Locations of adakitic lavas (open triangles) are grouped in blue rectangles. In general, the adakitic magmas erupted behind large exposures of forearc ophiolite.

Please cite this article as: Stern, C.R., Subduction erosion: Rates, mechanisms, and its role in arc magmatism and the evolution of the continental crust and mantle, Gondwana Res. (2011), doi:10.1016/j.gr.2011.03.006

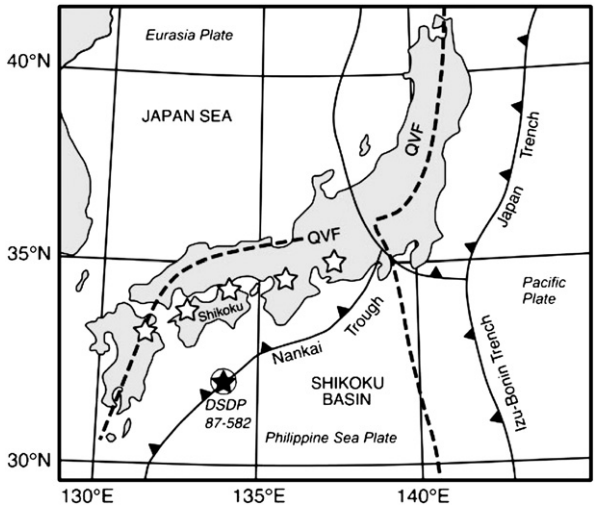

Fig. 21. Location of Setouchi volcanic belt (open stars) of high-Mg adakites, which extends for 600 km parallel to Nankai Trough and occupies the present forearc region, 80 km trenchward of the Quaternary volcanic front (QVF; Tatsumi, 2001). The Setouchi adakitic volcanic belt was active at 15–13 Ma, largely synchronous with timing of backarc-basin formation in Shikoku basin and Japan Sea in the early to middle Miocene. Subduction of a young and hot Philippine Sea plate beneath SW Japan resulted in partial melting of subducting slab, including forearc crust.

parallel belts of more typical calc-alkaline gabbro–diorite–granite batholiths, as a combination of decreasing subduction angle and subduction erosion of the forearc wedge leads to the landward migration of the locus of arc magmatism. The generation of these HiSY (for high Sr/Y; Tulloch and Kimbrough, 2003) arc magmas has been explained by melting of a deep mafic garnet–amphibolite or eclogite source, which could be either subducted oceanic crust, including subducted sediment, and/or mafic lower crust. In the case of the northern part of the La Posta suite of the Peninsula Range batholiths, Kimbrough and Grove (2006) and Grove et al. (2008) make the case that elevated $\delta^{18}O$ at intermediate $^{87}Sr/^{86}Sr$ values (0.704–0.708) cannot be accounted for by shallow level assimilation of the highly radiogeneic, early Mesozoic flysch host rocks. They explain these characteristics by partial melting and/or devolatilization of isotopically primitive low-grade metasedimentary and metavolcanic rocks and altered oceanic crust subducted into the source region. They suggest that subduction erosion delivered material similar to the Cataline Schist into the La Posta source region between 100 and 95 Ma. Devolatilization of this subducted sediment combined with asthenospheric corner flow above the hinge at which the subducting plate descended toward the mantle (Fig. 5) created the conditions to trigger the generation of the La Posta HiSY (TTG) suite. They determined that the La Posta plutons have elevated $\delta^{18}O$ only in the northern segment of the batholiths in southern California, where it was underplated by the Catalina Schists, and conclude that the process of subduction erosion that produced these schists was important in generating the source region characteristics of the La Post magmatic belt, which implies that a substantial fraction of subducted forearc material can be recycled via subduction erosion and incorporated into arc magmas over a relatively short (<10 my) time interval. A somewhat similar explanation has been proposed for the generation of Archean TTGs (Martin, 1986; Drummond and Defant, 1990; Rapp et al., 1991; Rapp and Watson, 1995), formed when terrestrial geothermal gradients were higher, slab-melting was more common, and subduction erosion may have operated at higher global rates as indicated by the scarcity of ancient, pre-Neoproterozoic blueschists (Stern, 2005, 2008; Brown, 2008; Condie and Kröner, 2008).

4.3. Summary

The mass balance calculations of Clift et al. (2009a) suggest that globally arc magmas contain ~20% of subducted forearc crust and sediment, which has therefore been recycled back into the crust by arc magmatism. Models that focus on primitive mantle-derived basalts in active arcs suggest even less recycling of subducted crust into arc magmas, generally <10%. Adakites and TTG suites may form by melting of subducted forearc crust, but globally adakites are relatively rare and form only during transient events of accelerated forearc erosion associated with changes in subduction geometry or subduction of buoyant features. Thus the compilations of Clift et al. (2009a) overestimate the current amount of recycling back into the crust of subducted forearc crust and sediment, and more of this material, >90% (>3.0 AU), is returned to the deep mantle than they suggest. More rapid subduction erosion, and more recycling though TTG arc magmas, might have occurred in the Archean and early Proterozoic.

5. Discussion

The information concerning subduction erosion reviewed above suggests that 1) for a long-term average over the last 150 Ma, more crust is subducted due to subduction erosion (>1.7 AU) than suggested in previous compilations (≤1.4 AU; Scholl and von Huene, 2007, 2009; Clift et al., 2009a, 2009b), which also implies that more total crust (~5.25 AU) is transported into the mantle than previously suggested (4.9 AU; Clift et al., 2009a, 2009b) by a combination of processes, including sediment subduction, continental lower crustal delamination, passive margin sediment subduction during continental collision, and loss of chemical solute, generated by weathering, that is dissolved in subducted oceanic crust; and also 2) less (<10%) of subducted sediment and forearc crust is returned to the crust in arc magmas than previously estimated (20%; Clift et al., 2009a). The implications for the growth and/or destruction of the continental crust, and the fate of the deeply subducted material (>3.0 AU), are discussed briefly below.

5.1. Subduction erosion and continental growth and/or destruction

Subduction erosion, sediment subduction, lower crustal delamination and subduction of continental crust associated with continental collision zones lead to a decrease in the total volume and potentially the partial destruction and disappearance of continents. Scholl and von Huene (2007, 2009), Clift et al. (2009a, 2009b) and Stern and Scholl (2010) review the rates of crustal loss to the mantle versus crustal additions due to arc and other magmatism, and the implications for the growth, preservation and/or destruction of the continental crust.

Scholl and von Huene (2007, 2009) restrict their discussion of crustal losses to subduction zone processes. They suggest that 2.5 AU of continental crust, consisting of sediment (1.1 AU) and forearc crust removed by subduction erosion (1.4 AU), are subducted into the mantle along convergent plate boundaries, and conclude that ≤10% of this is returned to the crust in arc magmas. Stern and Scholl (2010) make a similar estimate for subduction zone losses, and also included crustal loss at collision zones to add 0.7 AU, for a total crustal loss of 3.2 AU (Fig. 22A). Clift et al. (2009a, 2009b) consider forearc crust lost by subduction erosion to be 1.35 AU, sediment subduction to account for 1.65 AU, lower crustal delamination to be 1.1 AU, crustal loss at collision zones to be 0.4 AU, and loss of rock-weathering generated chemical solute that is dissolved in subducted oceanic crust to be 0.4 AU, for a total loss of continental crust equal to 4.9 AU (Fig. 22B). They consider that arc magmas contain 20% subducted sediment and forearc crust, which is thus returned to the crust and not recycled deeper into the mantle.

Please cite this article as: Stern, C.R., Subduction erosion: Rates, mechanisms, and its role in arc magmatism and the evolution of the continental crust and mantle, Gondwana Res. (2011), doi:10.1016/j.gr.2011.03.006

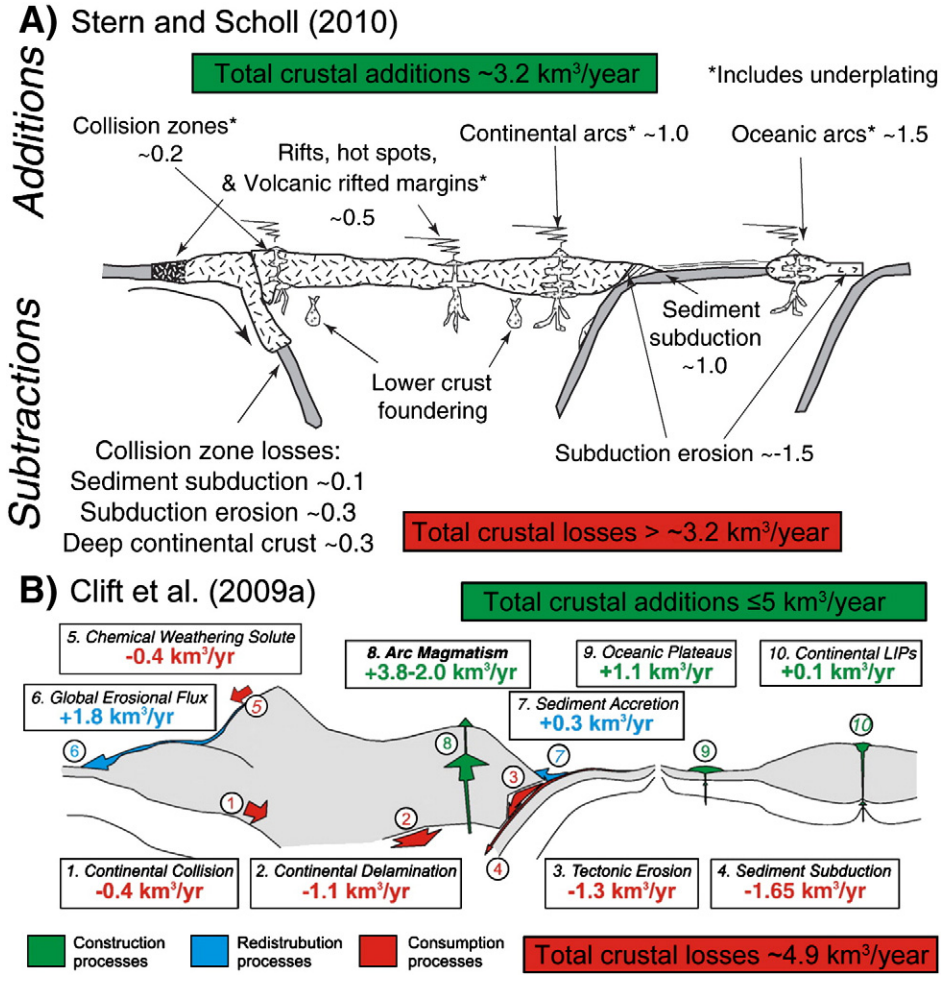

Fig. 22. Recent compilations by (A) Stern and Scholl (2010) and (B) Clift et al. (2009a) of different estimates of global rates of crustal losses and additions. The revised estimates made in this paper for both global long-term rates of subduction erosion of ~1.7 AU and total crustal losses of 5.25 AU are higher than crustal additions in either of their models.

Using the revised value of 1.7 AU estimated for the current long-term (<150 Ma) loss of forearc due to subduction erosion discussed above, and rates for the other processes of crustal losses as estimated by Clift et al. (2009a, 2009b), implies a higher total crustal loss rate of 5.25 AU. Combined with the lower estimated rates, discussed above, of only 10% of total subducted sediment and forearc crust being returned to the crust in arc magmas, the current total rate of recycling of crust into the deep mantle is here estimated to be >4.9 AU.

Stern and Scholl (2010) and Clift et al. (2009a, 2009b) also estimate the additions to the curst made by arc, hot-spot (oceanic islands, plateaus and continental LIPs), and continental collision magmatism (Fig. 22). Both conclude that in order to maintain the continental crust, oceanic island arcs, particularly in their early stages of formation, must have higher magma production rates than continental arcs, and that accretion of arcs to continental margins must be a relatively efficient process. However, Yamamoto et al. (2009) suggest that during arc–arc collision, in the case where the colliding arc is orthogonal to the other, the colliding arc will subduct into the mantle, together with the underlying oceanic lithosphere, without any evidence of accretion if the arc crust is <25 km thick. Only in the case where the two arcs are parallel with each other during collision will amalgamation take place. Even independent of this problem, the estimates of crustal additions by Stern and Scholl (2010), who conclude that currently more crust is likely being destroyed than created, are insufficient to account for the greater total crustal losses estimated by Clift et al. (2009a), and the estimates of Clift et al. (2009a), who also conclude that arc outputs are probably a little lower than needed to maintain the volume of the continental crust, are insufficient to account for the higher estimate of total global crustal losses in light of the higher long-term average of subduction erosion rates made here. Thus it appears that currently the continental crust is slowly shrinking, as originally suggested by Armstrong (1981, 1991).

Stern and Scholl (2010) and Santosh (2010) both make the point that crustal growth and destruction are not steady-state processes, but that their rates change over the period of supercontinent cycles, with crustal growth rates being greatest during supercontinent breakup, due to high magmatic fluxes, and crustal destruction being greatest during supercontinent amalgamation, due to increased sediment flux resulting from orogenic uplift (Stern and Scholl, 2010) as well as increased rates of subduction of continental material associated with super-downwelling resulting in double-sided subduction zones which swallow all intervening materials as the continents are pulled together into tight assemblies (Santosh et al., 2009). Current rates of subduction erosion and total global losses of continental crust therefore reflect only the current global tectonic environment in which the continents are widely dispersed.

5.2. Fate of the subducted crust

Continental crust is less dense than mantle, but the common occurrence of ultrahigh-pressure (UHP) metamorphic rocks in collisional orogenic belts suggests that subduction of even thick

Please cite this article as: Stern, C.R., Subduction erosion: Rates, mechanisms, and its role in arc magmatism and the evolution of the continental crust and mantle, Gondwana Res. (2011), doi:10.1016/j.gr.2011.03.006

sections of continental crust may reach depths of >300 km (Ye et al., 2000; Liou et al., 2002; Liu et al., 2007). Thus it also appears evident that some portions of the relatively thin continental materials within subduction channels may be subducted into the deep mantle. Geochemical studies on hotspot lavas report trace-element and isotopic data which indicate the presence of a recycled sediment (continental crust) component (White and Hofman, 1982; Phipps-Morgan and Morgan, 1999; Jackson et al., 2007; Workman et al., 2008), implying that sediment and/or forearc crust has been subducted into the deep mantle and subsequently entrained in upwelling plumes.

The transformations of plagioclase to jadeite (3.34 g/cm^3) + grossular (3.6 g/cm^3) + quartz (2.65), and quartz to stishovite (4.29 g/cm^3) at ~9 GPa, cause the zero-pressure density of model continental crust, similar in composition to tonalite–trondhjemite–granodiorite (TTG) granitoids, to jumps dramatically to 3.96 g/cm^3 (Fig. 23), thus allowing felsic crust to be subducted below the MOHO. Kawai et al. (2009) conclude that the zero-pressure density of TTG granitoids does not exceed that of pyrolite in the lower mantle and therefore subducted crustal material will remain above the mantle transition zone and not sink deeper into the lower mantle. In contrast, Komabayashi et al. (2009) suggest that at 22 GPa (660 km depth), TTG undergoes another decomposition reaction of jadeite to a Na–Al phase (NAL; 3.92 g/cm^3) + more stishovite, leading to another zero-pressure density jump of subducted continental crust from 3.96 to 4.21 g/cm^3 (Fig. 23). The study of UHP rocks also indicates that the subduction of continental crust is not controlled by its density alone, but by the net density of all the subducting materials, which for a subducting slab of oceanic crust consists of MORB as well as subducted sediment and forearc crust. Zero-pressure density of MORB reaches 4.29 g/cm^3 at 27 GPa (Hirose et al., 1999, 2005), compared to 4.19 g/cm^3 for pyrolite mantle (Fig. 23; Irifune and Ringwood, 1987). Also significant is that subducting materials are colder than the surrounding mantle, so that subducting continental crust and MORB will be denser than the surrounding mantle at all depths (Irifune and Ringwood, 1987). Komabayashi et al. (2009) therefore suggest that together with MORB, subducted TTG model continental crust could subduct into the lower mantle and accumulated in the D″ layer on the bottom of mantle (Fig. 24A). Thus they consider that the D″ layer is a chemically distinct region, the "anti-crust", composed of subducted continental crust, MORB and the mantle portion of past oceanic lithosphere.

The total volume of the ~275 km thick D″ layer is calculated to be 20 times more than that of the total volume of the current continental crust on the Earth, which suggests that over the course of Earth's history huge amounts of subducted oceanic lithosphere, including sediment and forearc continental crust similar to a model TTG continental crust, may have accumulated in the slab graveyard at the Core–Mantle Boundary (CMB; Senshu et al., 2009). Because subducted crust is enriched in K, U and Th, ca. 20 times more than that of CI chondrite meteorites, the anti-crust that accumulated in the D″ layer at the CMB during Archean and pre-Neoproterozoic times could have played a critical role to initiate the plumes or superplumes related to the origin of the superplume–supercontinent cycle (Senshu et al., 2009). When they initially accumulate, the temperature of subducted oceanic lithosphere is lower than overlying 'normal' mantle and the D″ layer is convectively stable. Eventually, due to the released heat from the decay of radioisotopes, this layer thermally expands and its density decreases so that a hot plume may form at the boundary between the D″ layer and overlying 'normal' mantle (Fig. 24B). Senshu et al. (2009) generate models of the thermal evolution of the D″ layer at different times in Earth history. In the case of 2 Ga, when heat production by radioactive decay in crustal materials is about 50% larger than that of present value, the D″ layer, initially assumed to be 200°K cooler than the overlying normal mantle, attains similar temperature as this overlying mantle in only 100 my, and by 200 my it becomes 250°K hotter than the overlying mantle, resulting in a thermally unstable plume.

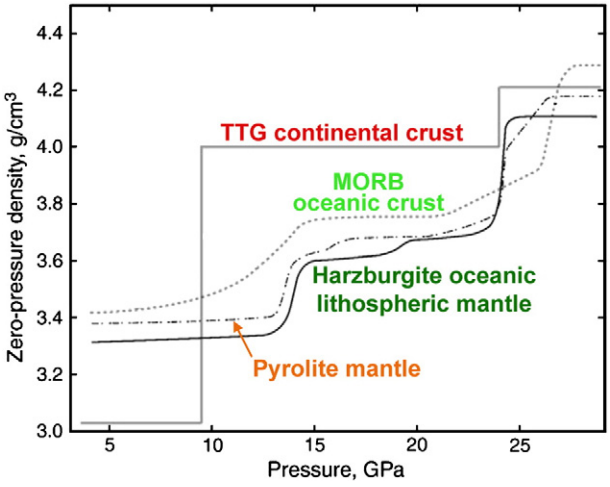

Fig. 23. Zero-pressure density profile to 27 GPa for TTG model continental crust subducted in the form of sediment (Komabayashi et al., 2009), MORB model oceanic crust (Irifune and Ringwood, 1987; Hirose et al., 1999, 2005), harzburgite model oceanic lithospheric mantle (Irifune and Ringwood, 1987), and mantle pyrolite (Irifune and Ringwood, 1987).

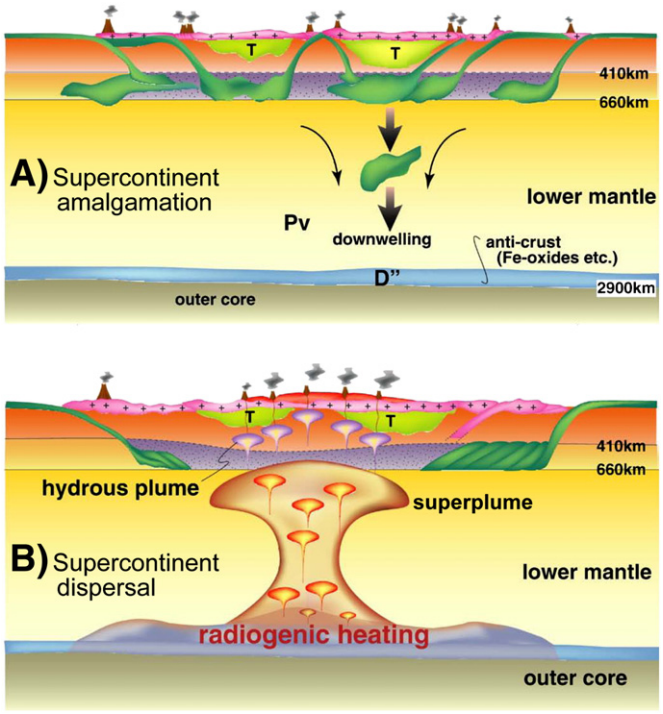

Fig. 24. A schematic cartoon, modified from Senshu et al. (2009), showing (A) deep subduction of oceanic lithosphere, including sediment and continental crust eroded by the subduction process, and the accumulation of the subducted slabs at either the 660 km discontinuity or possibly onto the core–mantle boundary; and (B) model of plume and superplume formation caused by accumulation and radiogenic heating of TTG "anti-crust" in the D″ slab graveyard layer. Crustal volume grows during continental dispersal and is reduced during continental amalgamation.

6. Conclusions

1) Subduction erosion occurs at all convergent plate margins. Globally it is responsible for returning >1.7 AU of crust back into the mantle, and is the most important among a number of processes that recycle at least 5.25 AU of crust back into the mantle.
2) Subduction erosion is not a steady-state process. Rates of subduction erosion depend on convergence rates, rates of sediment supply to

Please cite this article as: Stern, C.R., Subduction erosion: Rates, mechanisms, and its role in arc magmatism and the evolution of the continental crust and mantle, Gondwana Res. (2011), doi:10.1016/j.gr.2011.03.006

the trench, subduction angle and subduction of buoyant features such as seamount and oceanic ridges. Subduction erosion rates may have been higher in the remote past, and also depend on processes such as continental amalgamation associated with the supercontinent cycle.

3) Arc magmatism returns only a small (<10%) percent of subducted sediment and forearc crust back into the crust. The rest (>90%) is subducted deeper into the mantle.
4) Current rates of global crustal loss (5.25 AU) are greater than the rates of crustal additions, and the crust is currently shrinking. However, this is not a steady-state process, and long term rates of crustal growth and destruction depend on the supercontinent cycle.
5) Deeply subducted sediment and forearc crust may reach the 670 km discontinuity or may penetrate deeper into the lower mantle, perhaps as deep as the core–mantle boundary, along with subducted MORB. This processes replenished the mantle with radioactive elements to maintain the supercontinent cycle. Thus subduction erosion is a key process in maintaining global tectonic activity—it keeps the Earth cooking.

Acknowledgments

I wish to thank two anonymous reviewers for constructive comments that helped improve the final manuscript, Dan Mitchell for assistance in preparing the figures, and M. Santosh and T. Horscroft for inviting me to prepare this review.

References

Allmendinger, R., Jordan, T., Kay, S.M., Isacks, B., 1997. The evolution of the Altiplano-Puna plateau of the Central Andes. Annual Reviews on Earth and Planetary Sciences 25, 139–174.

ANCORP Working Group, 2003. Seismic image of a convergent continental margin and plateau in the central Andes. Journal of Geophysical Research 108 doi:10.1029/2002JB001771.

Armstrong, R.L., 1981. Radiogenic isotopes: the case for crustal recycling on a near-steady-state no-continental growth Earth. Royal Society of London Philosophical Transactions 301, 443–472.

Armstrong, R.L., 1991. The persistent myth of crustal growth. Australian Journal of Earth Sciences 38, 613–630.

Atherton, M.P., Petford, N., 1993. Generation of sodium-rich magmas from newly underplated basaltic crust. Nature 362, 144–146.

Atherton, M.P., Petford, N., 1996. Plutonism and the growth of Andean crust at 9 degrees S from 100 to 3 Ma. Journal of South American Earth Sciences 9, 1–9.

Bangs, N., Cande, S.C., 1997. Episodic development of a convergent margin inferred from structures and processes along the southern Chile margin. Tectonics 16, 489–503.

Bangs, N., Gulick, S.P.S., Shipley, T.H., 2006. Seamount subduction erosion in the Nankai Trough and its potential impact on the seismogenic zone. Geology 34, 701–704.

Barreiro, B.A., 1984. Lead isotopes and Andean magmagenesis. In: Harmon, R.S., Barreiro, B.A. (Eds.), Andean Magmatism; Chemical and Isotopic Constraints. : Shiva Geology Series. Shiva Publishing Limited, Natwich, UK, pp. 21–30.

Barth, A.P., Wooden, J.L., Grove, M.G., Jacobson, C.E., Pedrick, J.N., 2003. U–Pb zircon geochronology of rocks in the Salinas Valley region of California: a reevaluation of the crustal structure and origin of the Salinian block. Geology 31, 517–520.

Bindeman, I.N., Eiler, J.M., Yogodzinski, G.M., Tatsumi, Y., Stern, C.R., Grove, T., Portnyagin, M., Hoernle, K., Danyushevsky, L.V., 2005. Oxygen isotope evidence for slab melting in modern and ancient subduction zones. Earth and Planetary Science Letters 235, 480–496.

Bourgois, J., Pautot, G., Bandy, W., Boinet, T., Chotin, P., Huchon, P., Mercier de Lepinay, B., Monge, F., Monlau, J., Pelletier, B., Sosson, M., von Huene, R.W., 1988. Seabeam and seismic reflection imaging of the tectonic regime of the Andean continental margin off Peru (4°S to 10°S). Earth and Planetary Science Letters 87, 111–126.

Bourgois, J., Martin, H., Lagabrielle, Y., Le Moigne, J., Frutos, J., 1996. Subduction erosion related to spreading-ridge subduction: Taitao peninsula (Chile margin triple junction area). Geology 24, 723–726.

Bourgois, J., Guivel, C., Lagabrielle, Y., Calmus, T., Boulègue, J., Daux, V., 2000. Glacial–interglacial trench supply variation, spreading-ridge subduction, and feedback controls on the Andean margin development at the Chile triple junction area (45–48°S). Journal of Geophysical Research 105, 8355–8386.

Brown, M., 2008. Characteristic thermal regimes of plate tectonics and their metamorphic imprint throughout Earth history: when did Earth first adopt a plate tectonics mode of behavior? In: Condie, K.C., Pease, V. (Eds.), When did Plate Tectonics Begin on Planet Earth? : Geological Society of America Special Papers, 440, pp. 97–128.

Cande, S., Leslie, R.B., 1986. Late Cenozoic tectonics of the Southern Chile Trench. Journal of Geophysical Research 91, 471–496.

Chen, J.H., Moore, J.G., 1982. Uranium-lead isotopic ages from the Sierra Nevada batholith. Journal of Geophysical Research 87, 4761–4784.

Clift, P.D., Hartley, A., 2007. Slow rates of subduction erosion along the Andean margin and reduced global crustal recycling. Geology 35, 503–506.

Clift, P.D., Vannucchi, P., 2004. Controls on tectonic accretion versus erosion in subduction zones; implications for the origin and recycling of the continental crust. Reviews of Geophysics 42, RG2001 doi:10.1029/2003RG000127.

Clift, P.D., MacLeod, C.J., Tappin, D.R., Wright, D.J., Bloomer, S.H., 1998. Tectonic controls on sedimentation and diagenesis in the Tonga Trench and forearc, southwest Pacific. Geological Society of America Bulletin 110, 483–496.

Clift, P.D., Pecher, I., Kukowski, N., Hampel, A., 2003. Tectonic erosion of the Peruvian forearc, Lima Basin, by subduction and Nazca Ridge collision. Tectonics 22, 1023 doi:10.1029/2002TC001386.

Clift, P.D., Chan, L.-H., Blusztajn, J., Layne, G.D., Kastner, M., Kelly, R.K., 2005. Pulsed subduction accretion and tectonic erosion reconstructed since 2.5 Ma from the tephra record offshore Costa Rica. Geochemistry, Geophysics, Geosystems 6 doi:10.1029/2005GC000963.

Clift, P.D., Vannucchi, P., Morgan, J.P., 2009a. Crustal redistribution, crust–mantle recycling and Phanerozoic evolution of the continental crust. Earth-Science Reviews 97, 80–104.

Clift, P.D., Schouten, H., Vannucchi, P., 2009b. Arc–continent collisions, sediment recycling and the maintenance of the continental crust. In: Cawood, P.A., Kröner, A. (Eds.), Earth Accretionary Systems in Space and Time: Geological Society, London, Special Publications, 318, pp. 75–103.

Cloos, M., Shreve, R.L., 1988a. Subduction-channel model of prism accretion, mélange formation, sediment subduction, and subduction erosion at convergent plate margins, 1: background and description. Pure and Applied Geophysics 128, 456–500.

Cloos, M., Shreve, R.L., 1988b. Subduction-channel model of prism accretion, mélange formation, sediment subduction, and subduction erosion at convergent plate margins, 2: implications and discussion. Pure and Applied Geophysics 128, 501–545 doi:10.1007/BF00874549.

Coats, R.R., 1962. Magma type and crustal structure in the Aleutian arc. In: Macdonald, G.A., Kuno, H.Y. (Eds.), The Crust of the Pacific Basin, American Geophysical Union, Geophysics Monograph. Series 6, pp. 92–109.

Condie, K., Kröner, A., 2008. When did plate tectonics begin? Evidence from the geologic record. In: Condie, K.C., Pease, V. (Eds.), When did Plate Tectonics Begin on Planet Earth? : Geological Society of America Special Papers, 440, pp. 281–294.

Defant, M.J., Drummond, M.S., 1990. Derivation of some modern arc magmas by melting of young subducted lithosphere. Nature 347, 662–665.

Defant, M.J., Richerson, P.M., de Boer, J.Z., Stewart, R.H., Maury, R.C., Bellon, H., Drummond, M.S., Feigenson, M.D., Jackson, T.E., 1991. Dacite genesis via both slab melting and differentiation: petrogenesis of La Yeguada volcanic complex, Panama. Journal of Petrology 32, 1101–1142.

DeLong, S.E., Schwarz, W.M., Anderson, R.N., 1979. Thermal effects of ridge subduction. Earth and Planetary Science Letters 44, 239–246.

Drummond, M.S., Defant, M.J., 1990. A model for trondhjemite–tonalite–dacite genesis and crustal growth via slab melting: Archean to modern comparisons. Journal of Geophysical Research 95, 21503–21521.

Dumitru, T.A., Wakabayashi, J., Wright, J.E., Wooden, J.L., 2010. Early Cretaceous (ca. 123 Ma) transition from nonaccretionary behavior to strongly accretionary behavior within the Franciscan subduction complex. Tectonics doi:10.1029/2009TC002542.

Elliott, T., Plank, T., Zindler, A., White, W., Bourdon, B., 1997. Element transport from subducted slab to volcanic front at the Mariana Arc. Journal of Geophysical Research 102, 14991–15019.

Futa, K., Stern, C.R., 1988. Sr and Nd isotopic and trace element compositions of Quaternary volcanic centers of the Southern Andes. Earth and Planetary Sciences Letters 88, 253–262.

Goss, A.R., Kay, S.M., 2006. Steep REE patterns and enriched Pb isotopes in southern Central American arc magmas; evidence for forearc subduction erosion? Geochemistry, Geophysics, Geosystems 7 doi:10.1029/2005GC00116.

Gromet, L.P., Silver, L.T., 1987. REE variations across the Peninsula Ranges batholiths: implications for batholithic petrogenesis and crustal growth in magmatic arcs. Journal of Petrology 28, 75–125.

Grove, M., Jacobson, C.E., Barth, A.P., Vucic, A., 2003. Temporal and spatial trends of Late Cretaceous–early Tertiary underplating of Pelona and related schist beneath southern California and southwestern Arizona. In: Johnson, S.E., Patterson, S.R., Fletcher, J.M., Girty, G.H., Kimbrough, D.L., Martin-Barajas, A. (Eds.), Tectonic Evolution of Northwestern Mexico and the Southwestern USA: Geological Society of America Special Paper, 374, pp. 381–406.

Grove, M., Bebout, G.E., Jacobson, C.E., Barth, A.P., Kimbrough, D.L., King, R.L., Zou, H., Lovera, O.M., Mahoney, B.J., Gehrels, G.E., 2008. The Catalina Schist: evidence for middle Cretaceous subduction erosion of southwestern North America. In: Draut, A.E., Clift, P.D., Scholl, D.W. (Eds.), Formation and Applications of the Sedimentary Record in Arc Collision Zones: Geological Society of America Special Paper, 436, pp. 335–362.

Guivel, C., Lagabrielle, Y., Bourgois, J., Maury, R.C., Fourcade, S., Martin, H., Arnaud, N., 1999. New geochemical constraints for the origin of ridge-subduction-related plutonic and volcanic suites from the Chile Triple Junction (Taitao Peninsula and Site 862, LEG ODP 141 on the Taitao Ridge). Tectonophysics 311, 83–111.

Guivel, C., Lagabrielle, Y., Bourgois, J., Martin, H., Arnaud, N., Fourcade, S., Cotten, J., Maury, R.C., 2003. Very shallow melting of oceanic crust during spreading ridge subduction: origin of near-trench Quaternary volcanism at the Chile Triple Junction. Journal Geophysical Research 108, 2345 doi:10.1029/2002JB002119.

Please cite this article as: Stern, C.R., Subduction erosion: Rates, mechanisms, and its role in arc magmatism and the evolution of the continental crust and mantle, Gondwana Res. (2011), doi:10.1016/j.gr.2011.03.006

Gutscher, M.A., Maury, R., Eissen, J.P., Bourdon, E., 2000. Can slab melting be caused by flat subduction? Geology 28, 535–538.
Hampel, A., Adam, J., Kukowski, N., 2004a. Response of the tectonically erosive south Peruvian forearc to subduction of the Nazca Ridge: analysis of three-dimensional analogue experiments. Tectonics 23, TC5003 doi:10.1029/2003TC001585.
Hampel, A., Kukowski, N., Bialas, J., Huebscher, C., Heinbockel, R., 2004b. Ridge subduction at an erosive margin: the collision zone of the Nazca Ridge in southern Peru. Journal of Geophysical Research 109, B02101 doi:10.1029/2003JB002593.
Hartley, A.J., May, G., Chong, G., Turner, P., Kape, S.J., 2000. Development of continental forearc: a Cenozoic example from the Central Andes, northern Chile. Geology 28, 331–334.
Hickey, R., Frey, F., Gerlach, D., López-Escobar, L., 1986. Multiple sources for basaltic arc rocks from the Southern Volcanic Zone of the Andes (34°–41°S): trace element and isotopic evidence for contributions from subducted oceanic crust, mantle and continental crust. Journal of Geophysical Research 91, 5963–5983.
Hickey-Vargas, R., Moreno, H., López-Escobar, L., Frey, F., 1989. Geochemical variations in Andean basaltic and silicic lavas from the Villarrica-Lanín volcanic chain (39.5°S): an evaluation of source heterogeneity, fractional crystallization and crustal assimilation. Contributions to Mineralogy and Petrology 103, 361–386.
Hickey-Vargas, R., Sun, M., López-Escobar, L., Moreno, H., Reagan, M.K., Morris, J.D., Ryan, J.G., 2002. Multiple subduction components in the mantle wedge: evidence from eruptive centers in the Central Southern volcanic zone, Chile. Geology 30, 199–202.
Hilde, T.W.C., 1983. Sediment subduction versus accretion around the Pacific. Tectonophysics 99, 381–397.
Hildreth, W., Moorbath, S., 1988. Crustal contributions to arc magmatism in the Andes of central Chile. Contributions to Mineralogy and Petrology 103, 361–386.
Hirose, K., Fei, Y., Ma, Y., Mao, H.-K., 1999. The fate of subducted basaltic crust in the Earth's lower mantle. Nature 397, 53–56.
Hirose, K., Takafuji, N., Sata, N., Ohishi, Y., 2005. Phase transition and density of subducted MORB crust in the lower mantle. Earth and Planetary Science Letters 237, 239–251.
Irifune, T., Ringwood, A.E., 1987. Phase transformations in a harzburgite composition to 26 GPa: implications for dynamical behaviour of the subducting slab. Earth and Planetary Science Letters 86, 365–376.
Isozaki, Y., Aoki, K., Nakama, T., Yanai, S., 2010. New insight into a subduction-related orogen: a reappraisal of the geotectonic framework and evolution of the Japanese Islands. Gondwana Research 18, 82–105.
Ito, T., Kojima, Y., Kodaira, S., Sato, H., Kaneda, Y., Iwasaki, T., 2009. Crustal structure of southwest Japan, revealed by the integrated seismic experiment Southwest Japan 2002. Tectonophysics 472, 124–134.
Jackson, M., Hart, M.G., Koppers, S.R., Anthony, A.P., Staudigel, A.A.P., Konter, H., Blusztajn, J., Kurz, J., Russell, M., Jamie, A., 2007. The return of subducted continental crust in Samoan lavas. Nature 448, 684–687.
Jacobson, C.E., Barth, A.P., Grove, M., 2000. Late Cretaceous protolith age and provenance of the Pelona and Orocopia Schists, southern California: implications for evolution of the Cordilleran margin. Geology 28, 219–222.
Jacobson, C.E., Grove, M., Pedrick, J.N., Barth, A.P., Marsaglia, K.M., Gehrels, G.E., Nourse, J.A., 2011. Late Cretaceous–early Cenozoic tectonic evolution of the southern California margin inferred from provenance of trench and forearc sediments. Geologic Society of America Bulletin 123, 485–506.
Jordan, T., Isacks, B., Allmendinger, R., Brewer, J., Ramos, V.A., Ando, C.J., 1983. Andean tectonics related to geometry of the subducted Nazca Plate. Geological Society of America Bulletin 94, 341–361.
Kawai, K., Tsuchiya, T., Tsuchiya, J., Maruyama, S., 2009. Lost primordial continents. Gondwana Research 16, 581–586.
Kay, R.W., 1978. Aleutian magnesian andesites: melts from subducted Pacific Oceanic crust. Journal of Volcanology and Geothermal Research 4, 117–132.
Kay, R.W., 2006. Subduction erosion and recycled crust at convergent margins: the Adak adakite example. Geological Society America Penrose Conference on "Arc Genesis and Crustal Evolution", Valdez, Alaska, Abstracts, pp. 35–36.
Kay, S.M., Coira, B.L., 2009. Shallowing and steepening subduction zones, continental lithospheric loss, magmatism, and crustal flow under the Central Andean Altiplano-Puna Plateau. In: Kay, S.M., Ramos, V.A., Dickenson, W.D. (Eds.), Backbone of the Americas: Shallow Subduction, Plateau Uplift, and Ridge and Terrane Collision: Geological Society of America Memoirs, 204, pp. 229–259 doi:10.1130/2009.1204(11).
Kay, R.W., Kay, S.M., 2008. The Armstrong Unit (AU = km^3/yr) and Processes of Crust–Mantle Mass Flux. Goldschmitt 2008, Vancouver, Canada, Abstract A455.
Kay, S.M., Mpodozis, C., 2002. Magmatism as a probe to the Neogene shallowing of the Nazca plate beneath the modern Chilean flat-slab. Journal of South American Earth Sciences 15, 39–57.
Kay, R.W., Sun, S.S., Lee-Hu, C.N., 1978. Pb and Sr isotopes in volcanic rocks from the Aleutian Islands and Pribilof Islands, Alaska. Geochimica Cosmochimica Acta 42, 263–273.
Kay, R.W., Rubenstone, J.L., Kay, S.M., 1986. Aleutian terranes from Nd isotopes. Nature 322, 605–609.
Kay, S.M., Mpodozis, C., Ramos, V.A., Munizaga, F., 1991. Magma source variations for mid-late Tertiary magmatic rocks associated with a shallowing subduction zone and a thickening crust in the Central Andes (28-33°S). In: Harmon, R.S., Rapela, C.W. (Eds.), Andean Magmatism and Its Tectonic Setting. Geological Society of America Special Paper, 265, pp. 113–138.
Kay, S.M., Godoy, E., Kurtz, A., 2005. Episodic arc migration, crustal thickening, subduction erosion, and magmatism in the south-central-Andes. Geological Society of America Bulletin 117, 67–88.
Kilian, R., Stern, C.R., 2002. Constraints on the interaction between slab melts and the mantle wedge from adakite glass in peridotite xenoliths. European Journal of Mineralogy 14, 25–36.
Kimbrough, D.L., Grove, M., 2006. The eastern Peninsula Ranges batholithic flare-up: insights from zircon U–Pb ages and oxygen isotope ratios. Backbone of the Americas, Patagonia to Alaska. Geological Society of America Speciality Meeting, Mendoza, Argentina, Abstracts with Programs, 2, p. 107.
Komabayashi, T., Maruyama, S., Rino, S., 2009. Structure of D″ layer; anti-crust grown through 4.6 Ga subduction history of the earth. Gondwana Research 15, 342–353.
Kopf, A., 1999. Fate of sediment during plate convergence at the Mediterranean Ridge accretionary complex: volume balance of mud extrusion versus subduction and/or accretion. Geology 27, 87–90.
Kopf, A., Mascle, J., Klaeschen, D., 2003. The Mediterranean Ridge: a mass balance across the fastest growing accretionary complex on Earth. Journal of Geophysical Research 108, 2372 doi:10.1029/2001JB000473.
Kukowski, N., Oncken, O., 2006. Subduction erosion — the "normal" mode of fore-arc material transfer along the Chilean Margin. In: Oncken, O., Chong, G., Frantz, G., Giese, P., Gotze, H.J., Ramos, V.A., Strecker, M., Wigger, P. (Eds.), The Andes: Active Subduction Orogeny. Springer, pp. 217–236. Chapter 10.
Kulm, L.D., Schweller, W.J., Masias, A., 1977. A preliminary analysis of the geotectonic processes of the Andean continental margin, 6° to 45°S. In: Talwani, M., Pitman III, W.C. (Eds.), Island Arcs, Deep Sea Trenches and Back-arc Basins. : Maurice Ewing Symposium, 1. American Geophysical Union, pp. 285–301.
Kurtz, A.C., Kay, S.M., Charrier, R., Farrar, E., 1997. Geochronology of Miocene plutons and exhumation history of the El Teniente region, Central Chile (34–35°S). Revista Geológica de Chile 16, 145–162.
Lagabrielle, Y., Guivel, C., Maury, R.C., Bourgois, J., Fourcade, S., Martin, H., 2000. Magmatic–tectonic effects of high thermal regime at the site of active ridge subduction: the Chile Triple Junction model. Tectonophysics 326, 255–268.
Lagabrielle, Y., Suárez, M., Rossello, E.A., Hérail, G., Martinod, J., Régnier, M., Cruz, R., 2004. Neogene to Quaternary tectonic evolution of the Patagonian Andes at the latitude of the Chile Triple Junction. Tectonophysics 385, 211–241.
Lamb, S., Davis, P., 2003. Cenozoic climate change as a possible cause for the rise of the Andes. Nature 425, 792–797.
Laursen, J., Scholl, D.W., von Huene, R., 2002. Neotectonic deformation of the central Chile margin: deepwater forearc basin formation in response to hot spot ridge and seamount subduction. Tectonics 21 doi:10.1029/2001TC901023.
Liou, J.G., Zhang, R.Y., Katayama, I., Maruyama, S., 2002. Global distribution and petrotectonic characterizations of UHPM Terranes. In: Parkinson, C.D., Katayama, I., Liou, J.G., Maruyama, S. (Eds.), The Diamond-bearing Kokchetav Massif, Kazakhstan. Universal Academy Press, Inc., pp. 15–35.
Liu, L., Zhang, J.F., Green II, H.W., Jin, Z.M., Bozhilov, K.N., 2007. Evidence of former stishovite in metamorphosed sediments, implying subduction to ~350 km. Earth and Planetary Science Letters 263, 180–191.
Lohrmann, J., Kukowski, N., Krawczyk, C.M., Sick, C., Sobieski, M., Rietbrock, A., 2006. Subdcution channel evolution in brittle fore-arc wedges — a combined study with scaled sanbox experiments, seismological and reflection seismic data and geologic field evidence. In: Oncken, O., Chong, G., Frantz, G., Giese, P., Gotze, H.J., Ramos, V.A., Strecker, M., Wigger, P. (Eds.), The Andes: Active Subduction Orogeny. Springer, pp. 237–262. Chapter 1.
Macfarlane, A.W., 1999. Isotopic studies of northern Andean crustal evolution and ore metal sources. In: Skinner, B. (Ed.), Geology and Ore Deposits of the Central Andes: Society of Economic Geologists, Special Publication, 7, pp. 195–217.
Martin, H., 1986. Effect of steeper Archean geothermal gradients on geochemistry of subdcution zone magmas. Geology 14, 753–756.
Melnick, D., Echtler, H.P., 2006. Inversion of forearc basins in south-central Chile caused by rapid glacial age trench fill. Geology 34, 709–712.
Meschede, M., Zweigel, P., Kiefer, E., 1999. Subsidence and extension at a convergent plate margin: evidence for subduction erosion off Costa Rica. Terra Nova 11, 112–117.
Morris, J.D., Leeman, W.P., Tera, F., 1990. The subducted component in island arc lavas constraints from Be isotopes and B–Be systematics. Nature 344, 31–36.
Muñoz, J., Troncoso, R., Duhart, P., Crignola, P., Farmer, L., Stern, C.R., 2000. The relationship of the mid-Tertiary coastal magmatic belt in south-central Chile to the late Oligocene increase in plate convergence rate. Revista Geológica de Chile 27, 177–203.
Murauchi, S., 1971. The renewal of island arcs and the tectonics of marginal seas. In: Asano, S., Udintsev, G.B. (Eds.), Island Arc and Marginal Seas. Tokai University Press, Tokai, pp. 39–56.
Myers, J.D., Frost, C.D., Angevine, C.L., 1986. A test of the quartz eclogite source for parental Aleutian magmas: a mass balance approach. Journal of Geology 94, 811–828.
Nichols, G.T., Wyllie, P.J., Stern, C.R., 1994. Subduction zone melting of pelagic sediments constrained by melting experiments. Nature 371, 785–788.
Nichols, G.T., Wyllie, P.J., Stern, C.R., 1996. Experimental melting of pelagic sediments; constraints relevant to subduction. In: Bedout, G.E., Scholl, D.W., Kirby, S.H., Platt, J. P. (Eds.), Subduction Top to Bottom: American Geophysical Union Monograph, 96, pp. 293–298.
Pearce, J.A., Kempton, P.D., Nowell, G.M., Noble, S.R., 1999. Hf–Nd element and isotope perspective on the nature of provenance of mantle and subduction components in the western Pacific arc-basin systems. Journal of Petrology 40, 1579–1611.
Peterson, U., 1999. Magmatic and metallogenic evolution of the Central Andes. In: Skinner, B. (Ed.), Geology and Ore Deposits of the Central Andes: Society of Economic Geology Special Publication, 7, pp. 109–153.
Petford, N., Atherton, M., 1996. Na-rich partial melts from newly underplated basaltic crust: the Cordillera Blanca Batholith, Peru. Journal of Petrology 37, 1491–1521.

Please cite this article as: Stern, C.R., Subduction erosion: Rates, mechanisms, and its role in arc magmatism and the evolution of the continental crust and mantle, Gondwana Res. (2011), doi:10.1016/j.gr.2011.03.006

Phipps-Morgan, J., Morgan, W.J., 1999. Two-stage melting and the geochemical evolution of the mantle; a recipe for mantle plum-pudding. Earth Planetary Science Letters 170, 215–239.

Plank, T., Langmuir, C.H., 1993. Tracing trace elements from sediment input into volcanic output at subduction zones. Nature 362, 739–742.

Plank, T., Langmuir, C.H., 1998. The geochemical composition of subducting sediment and its consequences for the crust and mantle. Chemical Geology 145, 325–394.

Ranero, C.R., von Huene, R., 2000. Subduction erosion along the Middle America convergent margin. Nature 404, 748–752 doi:10.1038/35008046.

Rapp, R.P., Watson, E.B., 1995. Dehydration melting of metabasalt at 1–12 kbars: implications for continental growth and crust-mantle recycling. Journal of Petrology 36, 891–931.

Rapp, R.P., Watson, E.B., Miller, C.F., 1991. Partial melting of amphibolites/eclogite and the origin of Archean trondhjemites and tonalities. Precambrian Research 51, 1–25.

Rogers, G., Hawkesworth, C.J., 1989. A geochemical transverse across the North Chilean Andes: evidence of crust generation from the mantle wedge. Earth and Planetary Science Letters 91, 271–285.

Rutland, R.W.R., 1971. Andean orogeny and ocean floor spreading. Nature 233, 252–255.

Saleeby, J., 2003. Segmentation of the Laramide slab—evidence from the southern Sierra Nevada region. Geological Society of America Bulletin 115, 655–668.

Sallarés, V., Ranero, C.R., 2005. Structure and tectonics of the erosional convergent margin off Antofagasta, north Chile (23°30′S). Journal of Geophysical Research 110 doi:10.1029/2004JB003418.

Santosh, M., 2010. A synopsis of recent conceptual models on supercontinent tectonics in relation to mantle dynamics, life evolution and surface environment. Journal of Geodynamics 50, 116–133.

Santosh, M., Maruyama, S., Yamamoto, S., 2009. The making and breaking of supercontinents: some speculations based on superplumes, super downwelling and the role of tectosphere. Gondwana Research 15, 324–341.

Scheuber, E., Reutter, K.J., 1992. Magmatic arc tectonics in the Central Andes between 21° and 25°S. Tectonophysics 205, 127–140.

Schmitz, M., 1994. A balanced model of the southern Central Andes. Tectonics 13, 484–492.

Scholl, D.W., von Huene, R., 2007. Crustal recycling at modern subduction zones applied to the past — issues of growth and preservation of continental basement crust, mantle geochemistry, and supercontinent reconstruction. In: Hatcher, J.R.D., Carlson, M.P., McBride, J.H., Catalán, J.R.M. (Eds.), 4-D Framework of Continental Crust: Geological Society of America Memoir, 200, pp. 9–32.

Scholl, D.W., von Huene, R., 2009. Implications of estimated magmatic additions and recycling losses at the subduction zones of accretionary (non-collisional) and collisional (suturing) orogens. In: Cawood, P., Kröner, A. (Eds.), Accretionary orogens in space and time: Geological Society of London, Special Publication, 318, pp. 105–125.

Schweller, W.J., Kulm, L.D., 1978. Extensional rupture of oceanic crust in the Chile Trench. Marine Geology 28, 271–291.

Sen, C., Dunn, T., 1994. Dehydration melting of a basaltic composition amphibolites at 1.5 and 2.0 GPa: implications for the origin of adakites. Contributions to Mineralogy and Petrology 117, 394–499.

Senshu, H., Maruyama, S., Rino, S., Santosh, M., 2009. Role of tonalite–trodhjemite–granite (TTG) crust subduction on the mechanism of supercontinent breakup. Gondwana Research 15, 433–442.

Shimoda, G., Tatsumi, Y., Nohda, S., Ishizaka, K., Jahn, B.M., 1998. Setouchi high-Mg andesites revisited: geochemical evidence for melting of subducting sediments. Earth and Planetary Science Letters 160, 479–492.

Sigmarsson, O., Condomines, M., Morris, J.D., 1990. Uranium and ^{10}Be enrichments by fluids in Andean arc magmas. Nature 346, 163–165.

Sigmarsson, O., Martin, H., Knowles, J., 1998. Melting of a subducting oceanic crust from U–Th disequilibria in Austral Andean lavas. Nature 394, 566–569.

Sigmarsson, O., Chmeleff, J., Morris, J., López-Escobar, L., 2002. Origin of ^{226}Ra–^{230}Th disequilibria in arc lavas from southern Chile and implications for magma transfer time. Earth and Planetary Science Letters 196, 189–196.

Skewes, M.A., Holmgren, C., 1993. Solevantamiento Andino, erosión y emplazamiento de brechas mineralizadas en el depósito de cobre porfídico Los Bronces, Chile Central (33°S): aplicación de termometría de inclusiones fluidas. Revista Geológica de Chile 20, 71–84.

Stern, C.R., 1974. Melting products of olivine tholeiite basalt in subduction zones. Geology 2, 227–230.

Stern, C.R., 1989. Pliocene to present migration of the volcanic front, Andean Southern Volcanic Front. Revista Geológica de Chile 16, 145–162.

Stern, C.R., 1990. Comment on "A geochemical traverse across the northern Chilean Andes: evidence for crust generation from the mantle" by G. Rogers and C. Hawkesworth. Earth and Planetary Science Letters 101, 129–133.

Stern, C.R., 1991. Role of subduction erosion in the generation of the Andean magmas. Geology 19, 78–81.

Stern, C.R., 2004. Active Andean volcanism: its geologic and tectonic setting. Revista Geológica de Chile 31, 161–206.

Stern, R.J., 2005. Evidence from ophiolites, blueschists, and ultra-high pressure metamorphic terranes that the modern episode of subduction tectonics began in Neoproterozoic time. Geology 33, 557–560.

Stern, R.J., 2008. Modern-style plate tectonics began in Neoproterozoic time: an alternative interpretation of Earth's tectonic history. In: Condie, K.C., Pease, V. (Eds.), When did Plate Tectonics Begin on Planet Earth? : Geological Society of America Special Papers, 440, pp. 265–280.

Stern, C.R., Kilian, R., 1996. Role of the subducted slab, mantle wedge and continental crust in the generation of adakites from the Andean Austral Volcanic Zone. Contributions to Mineralogy and Petrology 123, 263–281.

Stern, C.R., Mpodozis, C., 1991. Geologic evidence for subduction erosion along the west coast of Central and Northern Chile. Actas 6th Congreso Geológico Chileno, Viña del Mar, pp. 205–207.

Stern, R.J., Scholl, D.W., 2010. Yin and yang of continental crust creation and destruction by plate tectonic processes. International Geology Review 52, 1–31.

Stern, C.R., Skewes, M.A., 1995. Miocene to Present magmatic evolution at the northern end of the Andean Southern Volcanic Zone, Central Chile. Revista Geológica de Chile 22, 261–272.

Stern, C.R., Wyllie, P.J., 1973. Melting relation of basalt–andesite–rhyolite–H_2O and a pelagic red clay at 30 kilobars. Contributions to Mineralogy and Petrology 42, 313–323.

Stern, T., Bateman, P.C., Morgan, B.A., Newell, M.F., Peck, D.L., 1981. Isotopic U–Pb Ages of Zircon from the Granitoids of the Central Sierra Nevada, California. U.S. Geological Survey Professional Paper 1185. 17 pp.

Stern, C.R., Frey, F.A., Futa, K., Zartman, R.E., Peng, Z., Kyser, T.K., 1990. Trace element and Sr, Nd, Pb and O isotopic composition of Pliocene and Quaternary alkali basalts of the Patagonian Plateau Lavas of southernmost South America. Contributions to Mineralogy and Petrology 104, 294–308.

Stern, C.R., Moreno, H., López-Escober, L., Clavero, J.E., Lara, L.E., Naranjo, J.A., Parada, M. A., Skewes, M.A., 2007. Chilean volcanoes. In: Moreno, T., Gibbons, W. (Eds.), The Geology of Chile. Geologic Society of London Press, pp. 149–180. Chapter 5.

Stern, C.R., Skewes, M.A., Arévalo, A., 2010. Magmatic evolution of the giant El Teniente Cu–Mo deposit, central Chile. Journal of Petrology doi:10.1093/petrology/egq029.

Stern, C.R., Floody, R., Espiñeira, D., 2011. Olivine–hornblende–lamprophyre dikes from Quebrada los Sapos, El Teniente, Central Chile (34°S): implications for the temporal geochemical evolution of the Andean subarc mantle. Andean Geology 38, 1–22.

Suárez, M., Bell, C.M., 1994. Braided rivers, lakes and sabkhas of the upper Triassic Cifuncho formation, Atacama region, Chile. Journal of South American Earth Sciences 7, 25–33.

Takagi, T., 2004. Origin of magnetite- and ilmenite-series granitic rocks in the Japan arc. American Journal of Science 304, 169–202.

Tatsumi, Y., 2001. Geochemical modeling of partial melting of subducting sediments and subsequent melt-mantle interaction: Generation of high-Mg andesites in the Setouchi volcanic belt, southwest Japan. Geology 29, 323–326.

Tera, F., Brown, L., Morris, J., Sacks, S.I., Klein, J., Middleton, R., 1986. Sediment incorporation in island-arc magmas: inferences from ^{10}Be. Geochimica Cosmochimica Acta 50, 535–550.

Tulloch, A.J., Kimbrough, D.L., 2003. Paired plutonic belts in convergent margins and the development of high Sr/Y magmatism: Peninsula Ranges Batholith of Baja California and Median Batholith of New Zealand. In: Johnson, S.E., Patterson, S.R., Fletcher, J.M., Girty, G.H., Kimbrough, D.L., Martin-Barajas, A. (Eds.), Tectonic Evolution of Northwestern Mexico and the Southwestern USA: Geological Society of America Special Paper, 374, pp. 275–295.

Vannucchi, P., Scholl, D.W., Meschede, M., McDougall-Reid, K., 2001. Tectonic erosion and consequent collapse of the Pacific margin of Costa Rica: combined implications from ODP Leg 170, seismic offshore data, and regional geology of the Nicoya Peninsula. Tectonics 20, 649–668.

Vannucchi, P., Ranero, C.R., Galeotti, S., Straub, S.M., Scholl, D.W., McDougall-Reid, K., 2003. Fast rates of subduction erosion along the Costa Rica Pacific margin: implications for nonsteady rates of crustal recycling at subduction zones. Journal of Geophysical Research 108, 2511 doi:10.1029/2002JB002207.

von Huene, R., Cullota, 1989. Tectonic erosion at the front of the Japan convergent margin. Tectonophysics 160, 75–90.

von Huene, R., Lallemand, S., 1990. Tectonic erosion along the Japan and Peru convergent margins. Geological Society of America Bulletin 102, 704–720.

von Huene, R., Ranero, C.R., 2003. Subduction erosion and basal friction along the sediment-starved convergent plate margin off Anatofagasta, Chile. Journal of Geophysical Research 108 doi:10.1029/2001JB001569.

von Huene, R., Scholl, D.W., 1991. Observations at convergent margins concerning sediment subduction, sediment erosion, and the growth of continental crust. Reviews of Geophysics 29, 279–316.

von Huene, R., Langseth, M., Nasu, N., Okada, H., 1982. A summary of Cenozoic tectonic history along the IPOD Japan trench transect. Geological Society of America Bulletin 93, 829–846.

von Huene, R., Suess, E., Leg 112 Shipboard Scientific Party, 1988. Ocean Drilling Program Leg 112, Peru continental margin, part 1, Tectonic history. Geology 16, 934–938.

von Huene, R., Corvalan, J., Flueh, E.R., Hinz, K., Korstgard, J., Ranero, C.R., Weinrebe, W., Scientists, Condor, 1997. Tectonic control of the subducting Juan Fernández Ridge on the Andean margin near Valparaiso, Chile. Tectonics 16, 474–488.

von Huene, R., Weinrebe, W., Heeren, F., 1999. Subduction erosion along the North Chile margin. Journal of Geodynamics 27, 345–358.

von Huene, R., Ranero, C., Vannucchi, P., 2004. Generic model of subduction erosion. Geology 32, 913–916.

Wells, R.E., Blakely, R.J., Sugiyama, Y., Scholl, D.W., Dinterman, P.A., 2003. Basin-centered asperities in great subduction zone earthquakes—a link between sip, subsidence and subduction erosion? Journal of Geophysical Research 108, 2507 doi:10.1029/2002JB002072.

White, W.M., Dupré, B., 1986. Sediment subduction and magma genesis in the Lesser Antilles: isotopic and trace element constraints. Journal of Geophysical research 91, 5927–5941.

White, W.M., Hofman, A.W., 1982. Sr and Nd isotope geochemistry of oceanic basalts and mantle evolution. Nature 296, 821–825 doi:10.1038/296821a0.

Woodhead, J.D., Fraser, D.G., 1985. Pb, Sr, and ^{10}Be isotopic studies of volcanic rocks from the Northern Mariana Islands: implications for magma genesis and crustal recycling in the western Pacific. Geochimica Cosmochimica Acta 49, 1925–1930.

Please cite this article as: Stern, C.R., Subduction erosion: Rates, mechanisms, and its role in arc magmatism and the evolution of the continental crust and mantle, Gondwana Res. (2011), doi:10.1016/j.gr.2011.03.006

Workman, R.K., Eiler, J., Hart, S.R., Jackson, M.G., 2008. Oxygen isotopes in Samoan lavas: confirmation of continent recycling. Geology 36, 551–554 doi:10.1130/G24558A.1.
Yamamoto, S., Senshu, H., Rino, S., Omori, S., Maruyama, S., 2009. Granite subduction: arc subduction, tectonic erosion and sediment subduction. Gondwana Research 15, 443–453.
Yáñez, G., Ranero, C., von Huene, R., Díaz, J., 2001. Magnetic anomaly interpretation across the southern Central Andes (32°–33.5°S): the role of the Juan Fernández ridge in the late Tertiary evolution of the margin. Journal of Geophysical Research 106, 6325–6345.
Yáñez, G., Cembrano, J., Pardo, M., Ranero, C., Selles, D., 2002. The Challenger–Juan Fernández–Maipo major tectonic transition of the Nazca–Andean subduction system at 33–34°S: geodynamic evidence and implications. Journal of South American Earth Sciences 15, 23–38.
Ye, K., Cong, B.L., Ye, D.N., 2000. The possible subduction of continental material to depths greater than 200 km. Nature 407, 734–736.
Yogodzinski, G.M., Volynets, O.N., Koloskov, A.V., Seliverstov, N.I., Matvenkov, V.V., 1994. Magnesian andesites and the subduction component in a strongly calc-alkaline series at Piip Volcano, far western Aleutians. Journal of Petrolology 35, 163–204.
Ziegler, A.M., Barret, S.F., Scotese, C.R., 1981. Paleoclimate, sedimentation and continental accretion. Royal Society of London Philosophical Transactions 301, 253–264.

Charles Stern is Professor in the Department of Geological Sciences at the University of Colorado in Boulder, Colorado. He received his Ph.D. from the University of Chicago in 1973, and spent four years as a Research Associate at Lamont-Doherty Geological Observatory of Columbia University before arriving in Colorado in 1979. His research interests include igneous petrology, volcanology, economic geology, cosmochemistry and geoarchaeology. Much of his research work is focused on igneous rocks and recent volcanic activity in the Patagonian Andes of southernmost South America.

Please cite this article as: Stern, C.R., Subduction erosion: Rates, mechanisms, and its role in arc magmatism and the evolution of the continental crust and mantle, Gondwana Res. (2011), doi:10.1016/j.gr.2011.03.006